



Leapfrogging into new territory

how Mascarene ridged frogs diversified across Africa and Madagascar to maintain their ecological niche

Zimkus, Breda M.; Lawson, Lucinda P.; Barej, Michael F.; Barratt, Christopher D.; Channing, Alan; Dash, Katrina M.; Dehling, J. Maximilian; Du Preez, Louis; Gehring, Philip-Sebastian; Greenbaum, Eli; Gvoždík, Václav; Harvey, James; Kielgast, Jos; Kusamba, Chifundera; Nagy, Zoltán T.; Pabijan, Maciej; Penner, Johannes; Rödel, Mark-Oliver; Vences, Miguel; Lötters, Stefan

Published in:

Molecular Phylogenetics and Evolution

DOI:

[10.1016/j.ympev.2016.09.018](https://doi.org/10.1016/j.ympev.2016.09.018)

Publication date:

2017

Document version

Publisher's PDF, also known as Version of record

Document license:

[CC BY-NC-ND](#)

Citation for published version (APA):

Zimkus, B. M., Lawson, L. P., Barej, M. F., Barratt, C. D., Channing, A., Dash, K. M., Dehling, J. M., Du Preez, L., Gehring, P-S., Greenbaum, E., Gvoždík, V., Harvey, J., Kielgast, J., Kusamba, C., Nagy, Z. T., Pabijan, M., Penner, J., Rödel, M-O., Vences, M., & Lötters, S. (2017). Leapfrogging into new territory: how Mascarene ridged frogs diversified across Africa and Madagascar to maintain their ecological niche. *Molecular Phylogenetics and Evolution*, 106, 254-269. <https://doi.org/10.1016/j.ympev.2016.09.018>



Leapfrogging into new territory: How Mascarene ridged frogs diversified across Africa and Madagascar to maintain their ecological niche



Breda M. Zimkus^{a,*}, Lucinda P. Lawson^b, Michael F. Barej^c, Christopher D. Barratt^d, Alan Channing^e, Katrina M. Dash^{f,g}, J. Maximilian Dehling^h, Louis Du Preez^{i,j}, Philip-Sebastian Gehring^k, Eli Greenbaum^f, Václav Gvoždík^{l,m}, James Harveyⁿ, Jos Kielgast^o, Chifundera Kusamba^p, Zoltán T. Nagy^{c,q}, Maciej Pabijan^r, Johannes Penner^{c,s}, Mark-Oliver Rödel^c, Miguel Vences^t, Stefan Lötters^u

^a Museum of Comparative Zoology, Harvard University, Cambridge, MA 02138, USA

^b Department of Biological Sciences, University of Cincinnati, 820F Rieveschl Hall, Cincinnati, OH 45221, USA

^c Museum für Naturkunde, Leibniz Institute for Evolution and Biodiversity Science, Invalidenstrasse 43, 10115 Berlin, Germany

^d University of Basel, Biogeography Research Group, Department of Environmental Sciences, Klingelbergstrasse 27, Basel 4056, Switzerland

^e University of the Western Cape, Biodiversity and Conservation Biology, Private Bag X17, Bellville 7535, South Africa

^f Department of Biological Sciences, University of Texas at El Paso, 500 W. University Ave., El Paso, TX 79968, USA

^g Department of Biology, Tidewater Community College, 120 Campus Dr., Portsmouth, VA 23701, USA

^h Institute of Integrated Sciences, Department of Biology, University of Koblenz-Landau, Universitätsstraße 1, 56070 Koblenz, Germany

ⁱ African Amphibian Conservation Research Group, Unit for Environmental Sciences and Management, North-West University, Potchefstroom 2520, South Africa

^j South African Institute for Aquatic Biodiversity, Somerset Street, Grahamstown 6139, South Africa

^k Fakultät für Biologie Universität Bielefeld, Abt. Biologiedidaktik, Universitätsstraße 25, 33615 Bielefeld, Germany

^l Institute of Vertebrate Biology, Czech Academy of Sciences, 603 65 Brno, Czech Republic

^m National Museum, Department of Zoology, 19300 Prague, Czech Republic

ⁿ Harvey Ecological, 35 Carbis Road, Pietermaritzburg 3201, KwaZulu-Natal, South Africa

^o Department of Biology, University of Copenhagen, Copenhagen, Denmark

^p Centre de Recherche en Sciences Naturelles, Département de Biologie, Lwiro, The Democratic Republic of the Congo

^q Joint Experimental Molecular Unit, Royal Belgian Institute of Natural Sciences, Rue Vautier 29, 1000 Brussels, Belgium

^r Department of Comparative Anatomy, Institute of Zoology, Jagiellonian University, Gronostajowa 9, 30-387 Kraków, Poland

^s Wildlife Ecology & Management, University of Freiburg, Tennenbacher Str. 4, 79106 Freiburg, Germany

^t Division of Evolutionary Biology, Zoological Institute, Technical University of Braunschweig, Mendelssohnstraße. 4, 38106 Braunschweig, Germany

^u Trier University, Department of Biogeography, 54286 Trier, Germany

ARTICLE INFO

Article history:

Received 2 June 2016

Revised 15 September 2016

Accepted 18 September 2016

Available online 21 September 2016

Keywords:

Amphibia

Historical biogeography

Pan-African

Phylogeny

Ptychadena

Species delimitation

Species distribution modeling

ABSTRACT

The Mascarene ridged frog, *Ptychadena mascareniensis*, is a species complex that includes numerous lineages occurring mostly in humid savannas and open forests of mainland Africa, Madagascar, the Seychelles, and the Mascarene Islands. Sampling across this broad distribution presents an opportunity to examine the genetic differentiation within this complex and to investigate how the evolution of bioclimatic niches may have shaped current biogeographic patterns. Using model-based phylogenetic methods and molecular-clock dating, we constructed a time-calibrated molecular phylogenetic hypothesis for the group based on mitochondrial 16S rRNA and cytochrome *b* (*cytb*) genes and the nuclear *RAG1* gene from 173 individuals. Haplotype networks were reconstructed and species boundaries were investigated using three species-delimitation approaches: Bayesian generalized mixed Yule-coalescent model (bGMYC), the Poisson Tree Process model (PTP) and a cluster algorithm (SpeciesIdentifier). Estimates of similarity in bioclimatic niche were calculated from species-distribution models (MAXENT) and multivariate statistics (Principal Component Analysis, Discriminant Function Analysis). Ancestral-area reconstructions were performed on the phylogeny using probabilistic approaches implemented in BioGeoBEARS. We detected high levels of genetic differentiation yielding ten distinct lineages or operational taxonomic units, and Central Africa was found to be a diversity hotspot for these frogs. Most speciation events took place throughout the Miocene, including “out-of-Africa” overseas dispersal

* Corresponding author.

E-mail addresses: bzimkus@oeb.harvard.edu (B.M. Zimkus), lucinda.lawson@uc.edu (L.P. Lawson), MichaelF.Barej@mfn-berlin.de (M.F. Barej), c.d.barratt@gmail.com (C.D. Barratt), achanning@uwc.ac.za (A. Channing), kmweber@miners.utep.edu, kdash@tcc.edu (K.M. Dash), dehling@uni-koblenz.de (J.M. Dehling), Louis.DuPreez@nwu.ac.za (L. Du Preez), SebastianGehring@web.de (P.-S. Gehring), egreenbaum2@utep.edu (E. Greenbaum), vaclav.gvozdik@ivb.cz (V. Gvoždík), info@harveyecological.co.za (J. Harvey), joskielgast@hotmail.com (J. Kielgast), chifkusamba@gmail.com (C. Kusamba), ztnagy@naturalsciences.be (Z.T. Nagy), maciej.pabijan@uj.edu.pl (M. Pabijan), johannes.penner@mfn-berlin.de (J. Penner), mo.roedel@mfn-berlin.de (M.-O. Rödel), m.vences@tu-braunschweig.de (M. Vences), loetters@uni-trier.de (S. Lötters).

<http://dx.doi.org/10.1016/j.ympev.2016.09.018>

1055-7903/© 2016 The Authors. Published by Elsevier Inc.

This is an open access article under the CC BY-NC-ND license (<http://creativecommons.org/licenses/by-nc-nd/4.0/>).

events to Madagascar in the East and to São Tomé in the West. Bioclimatic niche was remarkably well conserved, with most species tolerating similar temperature and rainfall conditions common to the Central African region. The *P. mascareniensis* complex provides insights into how bioclimatic niche shaped the current biogeographic patterns with niche conservatism being exhibited by the Central African radiation and niche divergence shaping populations in West Africa and Madagascar. Central Africa, including the Albertine Rift region, has been an important center of diversification for this species complex.

© 2016 The Authors. Published by Elsevier Inc. This is an open access article under the CC BY-NC-ND license (<http://creativecommons.org/licenses/by-nc-nd/4.0/>).

1. Introduction

Reconstructing the spatial and temporal history of organisms is one of the primary goals of evolutionary biology, yet obtaining a clear picture of evolutionary history can be challenging given that phylogenetics, species distributions, climatic history, and ecological processes, such as environmental tolerance and niche partitioning, must be taken into consideration (Wiens, 2011; Wiens and Graham, 2005). New methods are emerging that integrate ecological modeling, biogeographic reconstructions, and phylogenetic analyses to allow a more complete understanding of the contributions of geological and climatological phenomena, as well as ecological dimensions (Ahmadzadeh et al., 2016; Blair et al., 2015; Chan et al., 2011; Dowell and Hekkala, 2016; Rato et al., 2015). These methods also assist in the identification of important biogeographic boundaries, centers of speciation, and areas of extinction, which can be used in conjunction with species range information to make decisions regarding conservation of species and/or habitats.

The history of intra-African species diversification and expansion is poorly understood when contrasted with the well-studied phylogeography of the northern temperate zones, including Europe and North America. Very few datasets are available to evaluate African radiations, partially due to difficulties in sampling a sufficient number of populations across the vast Congo Basin, which is essential to reconstructing phylogenies and establishing range estimates for pan-continental lineages. Studies on diversification patterns of African lineages at a continental scale have almost exclusively focused on mammals and birds (Miller et al., 2010a; Njabo et al., 2008; Outlaw et al., 2007; Smitz et al., 2013), while large-scale data are available for few reptiles and amphibians. More specifically, the evolutionary history of many savannah mammals has been well studied, including ungulates, which show colonization patterns from north to east and east to north from isolated Pleistocene savannah refugia (Lorenzen et al., 2012). Studies on the diversification of non-mammalian African vertebrates support a variety of expansion patterns that are more influenced by pre-Pleistocene geological and climatic factors. Avian studies implicate Pliocene forest dynamics as the driving force generating biodiversity, with forest retraction allowing arid-adapted species to colonize southern Africa (Guillaumet et al., 2008; Outlaw et al., 2007; Voelker et al., 2010). Lizards of the *Agama agama* complex diversified in the Miocene with expansion southwards from populations in either North or West Africa (Leaché et al., 2014). *Panaspis* skinks, generally occurring in non-forested habitats of sub-Saharan Africa, also exhibited a pattern of Miocene diversification with the most basal divergences separating members from West Africa from others (Medina et al., 2016). African amphibian radiations, which are most often endemic to the continent as a result of low vagility, are particularly poorly understood. Some frog lineages appear to have originated in Central Africa, including the most recent common ancestor to the arthroleptid genera *Arthroleptis* and *Cardioglossa* (Blackburn, 2008), as well as the subgenus *Silurana* (Evans et al., 2004), whereas others have an eastern origin, including the subgenus *Xenopus* (Evans et al., 2004) and the

genus *Phrynobatrachus* (Zimkus et al., 2010). To date, no study has integrated biogeography and species distribution modeling to examine diversification of an amphibian clade with a Pan-African distribution.

The *Ptychadena mascareniensis* species complex is an ideal model system to evaluate the processes of speciation, diversification, and bioclimatic niche evolution within a pan-continental radiation, as members of this complex are found across the entire sub-Saharan region and along the Nile River in Egypt and Sudan (Frost, 2016). In addition, this species complex is widely distributed across Madagascar and other islands within the Indian Ocean, so it presents a unique opportunity to investigate patterns of diversification on contrasting ecological landscapes. The *P. mascareniensis* complex includes: (1) *P. mascareniensis* sensu lato distributed across Madagascar, the Seychelles and Mascarene Islands, including at least two deeply divergent lineages, (2) *P. cf. mascareniensis* distributed across Africa, including at least four deeply divergent lineages, (3) *P. nilotica*, widely distributed across eastern sub-Saharan Africa and Nilotic Egypt, (4) *P. filwoha*, restricted to the Rift Valley of Ethiopia, and (5) *P. newtoni*, endemic to São Tomé in the Gulf of Guinea (Dehling and Sinsch, 2013; Frost, 2016; Measey et al., 2007; Vences et al., 2004). Previous phylogenetic studies have focused on understanding transoceanic dispersal within this complex of frogs (Measey et al., 2007; Vences et al., 2004), but the potentially important role of the environment in shaping speciation has not yet been investigated. Widespread sampling across the broad distribution of this complex allows a more in-depth re-examination of the intraspecific genetic differentiation within this complex.

In this study, we use a multilocus dataset to infer phylogenetic relationships, investigate species boundaries, estimate divergence times, and reconstruct the historical biogeography of the complex. We investigate previously recognized lineages and biogeographic patterns (Dehling and Sinsch, 2013; Vences et al., 2004), but we hypothesize that increased sampling and enhanced species delimitation will lead to the identification of cryptic species and resolve the relationships among lineages. We combine phylogenetic data with spatial environmental variables and multivariate statistical analyses to (1) predict the distribution of each lineage based on georeferenced occurrence records and bioclimatic variables under current and past climatic conditions and (2) estimate similarity and evolution of bioclimatic envelopes. The combination of dated phylogenetic information and species distribution models gives us insight into whether niche conservatism and/or differentiation has contributed to current distributions. Our analyses aim to provide insights into the evolutionary history of the *P. mascareniensis* complex and to determine whether patterns of niche conservatism or divergence dominate in this complex of frogs.

2. Materials and methods

2.1. Taxonomy and terminology

Representatives of all lineages previously identified within the *Ptychadena mascareniensis* complex are included in our analyses:

P. mascareniensis (Madagascar), *P. mascareniensis* B–E (sensu Measey et al., 2007; Vences et al., 2004), *P. filwoha*, *P. nilotica* (identified as *P. mascareniensis* A by Vences et al. (2004) and Measey et al. (2007)), and *P. newtoni* (Dehling and Sinsch, 2013; Measey et al., 2007; Vences et al., 2004). We refer to genealogical units at or below the species level as lineages, and those lineages supported by the species delimitation approaches (see below) are here termed operational taxonomic units (OTUs) (Blaxter et al., 2005). In addition, we use the term “cluster” to denote cohesive taxonomic units identified through species delimitation approaches (see below).

2.2. Sample collection

Specimens were collected during visual encounter surveys (daytime), and acoustic encounter surveys (night). Voucher specimens were anesthetized and euthanized, sampled for tissue (liver/muscle), fixed with formalin and stored in 70% ethanol. Individuals that were not collected as vouchers were sampled (toe clip) and released. All liver or muscle tissue samples were stored in 99% ethanol. Representative voucher specimens were collected and deposited in the herpetological collections of various museums; abbreviations correspond to those of Sabaj (2016) with the addition of AACRG (African Amphibian Conservation Research Group

based at North-West University, South Africa). Additional abbreviations refer to field numbers of C.D. Barratt (CB), A. Channing (AC), J.M. Dehling (JMD), P.-S. Gehring (PSG), F. Glaw (FGZC), E. Greenbaum (ELI), V. Gvoždík (VG), Z.T. Nagy (A, CRT, KG), M. Pabijan (MPFC), J. Penner (JP) and M. Vences (ZCMV). Geographic coordinates were recorded with GPS receivers. Fig. 1 and Table S1 provide information on GPS coordinates of sampling locations.

2.3. DNA extraction and amplification

DNA was extracted from tissue samples using Qiagen DNeasy tissue kits (Qiagen Inc., Hilden, Germany). Fragments of the mitochondrial 16S ribosomal RNA (16S) and cytochrome *b* (*cytb*) genes, as well as a fragment of the nuclear Recombination Activating Gene 1 (*RAG1*), were amplified by polymerase chain reaction (PCR). The sequences of the primers are included in Table S2. Amplification followed standard PCR conditions (Palumbi, 1996) with the following thermal cycle profile: 2 min at 94 °C, followed by 35 cycles of 94 °C for 30 s, 46 °C for 30 s, and 72 °C for 60 s, and a final extension phase at 72 °C for 7 min. All amplified PCR products were verified using electrophoresis on a 1.0% agarose gel stained with SYBR Safe DNA gel stain (Invitrogen Corporation, Carlsbad, CA, USA). PCR products were purified using the Qiagen DNeasy DNA Purification System according to the manufacturer's

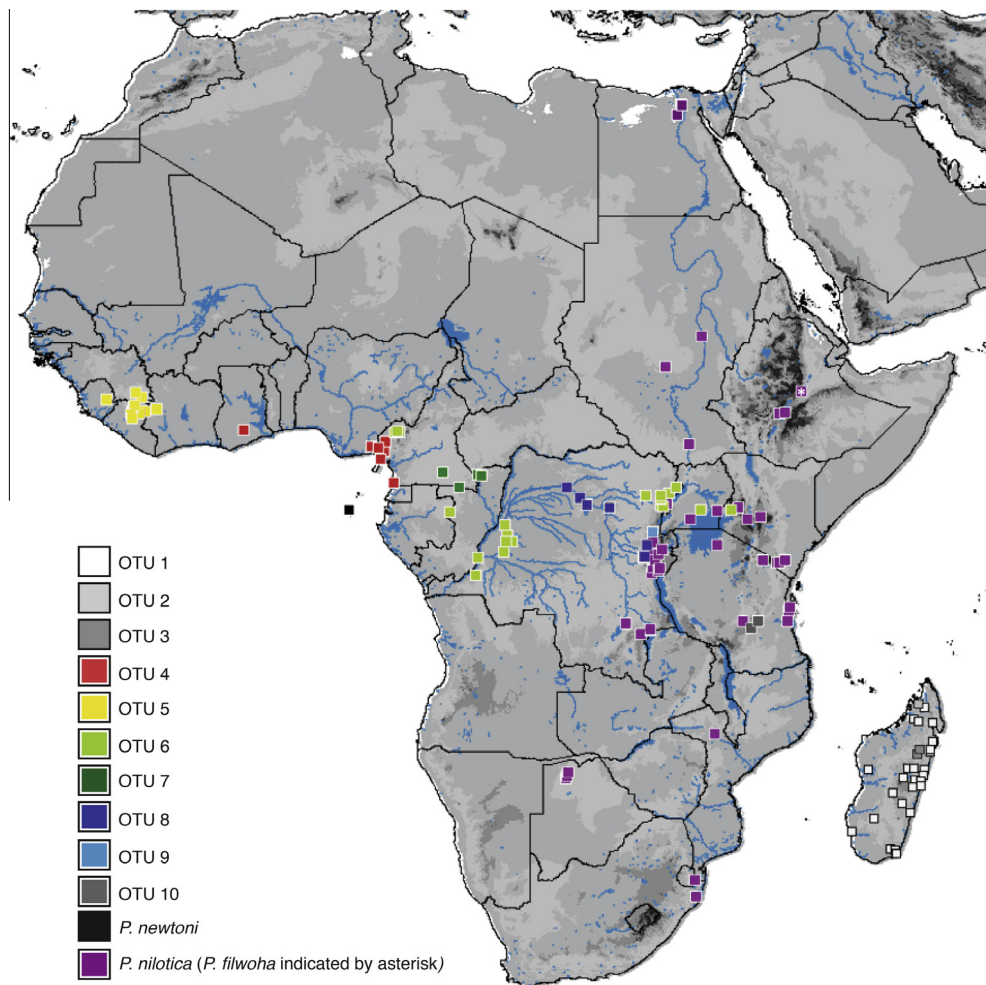


Fig. 1. Occurrences of *Ptychadena mascareniensis* lineages identified in this study. *Ptychadena mascareniensis* sensu lato includes OTUs 1–3. Seven putative candidate species from Africa are identified (OTUs 4–10). Lineages identified within Africa are outlined in white, while those on islands (Madagascar in the East and São Tomé in the West) are not outlined. For purposes of this study, *P. nilotica* includes *P. filwoha*, indicated by a white asterisk. For interpretation of the references to color in this figure, the reader is referred to the web version of this article.

recommendations. DNA sequencing was done on an automated DNA sequencer (ABI PRISM 3730xl). All three gene fragments were sequenced in both directions. Sequences were checked for reliability using the original chromatograph data, and assembly of contigs was completed in Sequencher 5.0 (Gene Codes Corp., Ann Arbor, MI, USA) and CodonCode Aligner (v. 2.0.6, Codon Code Corporation). Sequences were aligned using Clustal Omega (Sievers et al., 2011) and confirmed by eye. New sequences generated from this study (173 individuals) were compiled with previously published sequence data (Table S1). Based on preliminary analyses of the entire genus (B.M. Zimkus, unpublished), only those species within the clade of interest (*P. cf. mascareniensis*, *P. mascareniensis*, *P. filwoha*, *P. newtoni*, *P. nilotica*) were included; *Ptychadena pumilio* and *P. submascareniensis* were used to root the tree(s). Protein-coding partitions of mitochondrial and nuclear genes (*cytb*, *RAG1*) were translated to amino acids using the program Translator X (Abascal et al., 2010) to set codon positions and to confirm absence of stop codons. Polymorphic positions in *RAG1* were coded as heterozygotes. DnaSP v5 (Librado and Rozas, 2009) was used to phase *RAG1* data and infer haplotypes. A total of 124 out of the 152 *RAG1* sequences (82%) could be phased with high certainty (>0.8); the remaining 28 sequences (18%) were phased with probabilities <0.8. Sequence lengths of each locus were as follows: 512 bp of *16S*, 602 bp of *cytb*, 644 bp of *RAG1* (reduced to 589 bp after removing missing data). Percent pairwise uncorrected molecular distances between species were calculated using PAUP* 4b10 (Swofford, 2001). All novel nucleotide sequence data were deposited in GenBank (accession numbers KX836389–KX836865).

2.4. Phylogenetic reconstruction and divergence-time estimation

PartitionFinder 1.1.1 (Lanfear et al., 2012) was used to determine the best-fitting partition scheme and models of molecular evolution according to the Bayesian information criterion. The program suggested a total of five partitions for use with MB and four partitions for use with BEAST; models of nucleotide substitution are provided in Table S3.

Estimates of phylogeny were obtained for both single genes and a concatenated dataset using maximum likelihood (ML) and Bayesian inference performed on the CIPRES Science Gateway (Miller et al., 2010b), and in BEAST 1.8.2 (Heled and Drummond, 2010). The ML analyses were conducted in RAxML version 8.1.24 (Stamatakis, 2014) using the rapid hill-climbing algorithm and the GTRGAMMA substitution model. Bayesian inference was performed with MrBayes (MB) version 3.2.2 (Ronquist et al., 2012) implementing two parallel runs of four simultaneous Markov chains for 10 million generations, sampling every 1000 generations and using the default parameters. The first one million generations (10%) were discarded as burn-in, based on stationarity of the log-likelihood tree scores. Nodal support was evaluated by non-parametric bootstrapping with 1000 replicates performed with RAxML (ML), and by posterior probabilities (MB). Topologies present in at least 70% of bootstrap trees were considered well supported (Hillis and Bull, 1993), whereas posterior probabilities ≥ 0.95 were considered well supported (Wilcox et al., 2002).

BEAST 1.8.2 was used to obtain a mitochondrial phylogeny for species delimitation with bGMYC and to use as a guide for *BEAST species tree analyses. Suitable calibration points were not available for the evolutionary history of the ingroup; therefore, we relied on previously published mutation rates (rate of change per lineage per million years) from various lizard groups for the combined mitochondrial genes (0.0125/Myr; middle of range of 0.0115–0.0135; Miralles and Carranza, 2010) and amphibians for the *RAG1* gene (0.00042/Myr; Evans et al., 2008). Uncorrelated lognormal relaxed clocks were used for both mitochondrial and nuclear loci. The BEAST analysis was run for 150 million generations with sampling

every 1000. The first 10% of generations were discarded as burn-in based on examination of parameter convergence in Tracer 1.6 (Rambaut, 2014b). In the final tree, ESS values were above 200 and effective mixing was achieved.

2.5. Haplotype networks and species delimitation

Haplotype networks were constructed for each gene using the algorithm of Templeton et al. (1992) and implemented in TCS 1.21 with a connection limit of 95% confidence criteria (Clement et al., 2000; Templeton et al., 1992). The genetic diversity within the *Ptychadena mascareniensis* complex was examined, and species boundaries were estimated using three different approaches. In approach 1, OTUs were assessed on the basis of the mitochondrial genes *16S* and *cytb* with the software TaxonDNA 1.7 and the implemented 'Cluster' algorithm in SpeciesIdentifier (Meier et al., 2006). This method considers overlaps between intra- and interspecific variation, and the maximum pairwise distance within recognized OTUs (a putative species-level criterion) should not exceed a given threshold. OTUs, herein termed clusters, are identified according to pairwise (uncorrected) distances for sequences within each cluster. We reduced the dataset to unique haplotypes for each gene. Incremental values ranged from 1.0% with an increase of 0.5% in each step, to a maximum of 5.0% in *16S* and 6.0% in *cytb*. The remaining two approaches used for inferring species boundaries were based on differences in branching rates at species and population levels, assuming that the number of substitutions within a species is significantly lower than between species. For approach 2, we analyzed the concatenated mitochondrial dataset (*16S*, *cytb*) using the Bayesian generalized mixed Yule coalescence (bGMYC; Fujisawa and Barraclough, 2013). A Bayesian general mixed Yule-coalescent (bGMYC) model was implemented in the bGMYC package in R v.3.2.1 using 100 random trees from the BEAST analysis. Simulations were set at 50,000 generations with 40,000 burn-in, sampling every 100th generation. The results of bGMYC analyses were then summarized with a probability matrix plot, and clades with $P > 0.7$ were interpreted as significant genetic differentiation in light of accompanying distributional data. This probability value threshold represents the best estimate of species limits given the bGMYC model and our sequence data, signifying a compromise between failing to recognize true species and recognizing false species. In contrast to bGMYC, which uses time to simulate speciation and coalescent events, the Poisson tree processes model (PTP) uses the number of substitutions, and species delimitations are based on heuristic search algorithms to estimate species boundaries with maximum-likelihood scores (Zhang et al., 2013). In approach 3, PTP analyses were conducted on the bPTP webserver (<http://species.h-its.org/ptp/>) using the RAxML tree of the concatenated dataset of all three genes (*16S*, *cytb* and *RAG1*) as input data (outgroups removed before analysis) with 500,000 MCMC generations, thinning set to 100, burnin at 25% and performing a Bayesian search. The probability of each node to represent a species node was calculated using the maximum-likelihood solution.

2.6. Species tree

Following species delimitation, a *BEAST (Heled and Drummond, 2010) species tree was constructed using the phylogenetically identified OTUs. As the automated species-delimitation methods (bGMYC, PTP) achieved similar results but tended to overestimate the number of potential species for some lineages, we used results of clustering analyses (SpeciesIdentifier) to designate OTUs. All genes had separate substitution models; however, the mtDNA data were linked into a single-tree model, and all phased *RAG1* sequences were linked into a second tree for the

species-tree estimation. As in the BEAST analyses, a relaxed lognormal clock was used for all loci. Two independent runs of 100 million generations, sampling every 1000 generations, was assessed for stability. The first 30% were discarded as burn-in for both convergence and tree estimates. Site models and clocks were the same as above (BI models). A Yule-species tree model with piecewise linear population-size growth with constant root was used. Convergence was assessed using Tracer through a visual inspection of adequate mixing and ESS estimates >200. The maximum clade credibility tree was calculated using TreeAnnotator 1.7.5. The final trees were visualized with FigTree 1.4.2 (Rambaut, 2014a).

2.7. Species distribution modeling

Species Distribution Models (SDM, also known as Ecological Niche Models, ENM) for OTUs 1, 4, 5, 6, 8 and *P. nilotica* were built based on known presence records and climatic information (Peterson et al., 2011). All remaining lineages had occurrence records below the threshold of $n = 10$ for reliable model estimation and were not used. For details on records of modeled *Ptychadena* with georeferenced latitude-longitude information see Table S1. In our approach, we used grid-based ‘bioclim’ variables (Table S4) at resolution of 30 arc-sec, derived from WorldClim (Hijmans et al., 2005) for the period 1950–2000; data were downloaded from <http://www.worldclim.org>. Bioclim variables are latitude-independent and suggested to possess a higher biological relevance than raw climatic information (Beaumont et al., 2005; Busby, 1991). In the ‘classical’ way, they are widely used in ecological modeling to reflect temperature (bio1–11) and precipitation (bio12–19) regimes (Booth et al., 2014). To avoid multicollinearity in ecological space (Heikkinen et al., 2006), we reduced the set of bioclim variables to six layers defining the availability of thermal energy and water (e.g. the minimum, maximum, and mean values at the species records): bio1, 5, 6, 12, 13, 14 were chosen based on their use in previous analyses (Table S4; Ficetola et al., 2007; Peterson et al., 2008). To obtain information on potential distributions of *Ptychadena* lineages during historical wet and dry climatic extremes (i.e., the Last Glacial Maximum (LGM, ca. 22,000 years ago), and the Last Interglacial (LIG, ca. 120,000–140,000 years ago), we projected SDMs to past climatic conditions (Peterson et al., 2011). LGM and LIG models were generated using General Circulation Model simulations from the Community Climate System Model (CCSM), downscaled and bias-corrected using WorldClim. Data are available from <http://www.worldclim.org> and were translated into bio1–19. We used MAXENT 3.3.3k for the calculation of SDMs, which employs a machine-learning algorithm based on the principles of maximum entropy (Phillips et al., 2006; Phillips and Dudík, 2008), and has been shown to be highly effective at predicting distributions with presence-only data (i.e., no absence records) (Elith et al., 2006, 2011). MAXENT particularly outperforms other algorithms when the number of presence records is relatively low (Hernandez et al., 2006), as in OTU 4. We employed MAXENT under default settings (but excluded ‘product features’ in model computation; Merow et al., 2013) using ‘bootstrap’ with 10 iterations to average model output and 10,000 background points. Background was individually defined for each OTU or species based on the known records. We chose MAXENT’s logistic output format (ranging 0–1) when deriving SDMs for predicted bioclimatic suitability on the African continent. Following Phillips et al. (2006), the non-fixed ‘minimum training presence logistic threshold’ was taken for discriminating species presence versus absence and when mapping MAXENT output. In MAXENT, the Area Under the Curve (AUC) can be calculated, a standard measure to assess model performance in statistical ecology (Phillips et al., 2006). For this purpose, 25% of all records were excluded from model training but used for posterior model testing. AUCs range

from 0.5 (not predictive of model) to 1.0 (perfect prediction of model); values >0.9 describe ‘very good’, >0.8 indicate ‘good’, and >0.7 designate ‘useable’ model discrimination abilities (Araújo et al., 2005; Swets, 1988).

2.8. Overlap of bioclimatic envelope and range size

We applied both Discriminant Function Analysis (DFA) and Principal Component Analysis (PCA) using bioclim variables associated with GPS coordinates (Tables S1 and S4) to approximate similarity of bioclimatic envelope across lineages with a large number of limited-distribution lineages (<5 GPS coordinates per species). All analyses were performed in the R statistical environment version 3.2.3 (R Core Development Team, 2014) with ‘MASS,’ ‘ggord,’ ‘ggplot2,’ and ‘ggbiplot’ packages (V.Q. Vu, <https://github.com/vqv/ggbiplot>; Venables and Ripley, 2002; Wickham, 2009). The inertia ellipses (95%) are shown for each species with sufficient points to assess overlap of bioclimatic envelopes. This method allows an assessment of bioclimatic similarity for severely range-restricted taxa, such as many members of this complex. All 19 standard bioclim variables (30 arc-sec resolution, WorldClim; Hijmans et al., 2005) were included in the analyses, and the calculation was performed at multiple resolutions on the phylogenetic tree to prevent distantly related species with divergent bioclimatic envelopes from swamping the signal of more closely related lineages.

Sister lineages OTU 4 and OTU 5 had sufficient sampling for MAXENT analysis, and significantly different bioclimatic niches (DFA analysis, results); thus, we were able to evaluate bioclimatic divergence between these lineages in more detail than other lineages within this system. Bioclimatic similarity was assessed in SDMtools v. 1.4.4 (Warren et al., 2010; Warren and Seifert, 2011) comparing overlap between these two adjacent but allopatric species to background tests using a common background area encompassing the range of these species (polygon with coordinates of latitude 12° to 0°, longitude –14° to 12°) with 100 replicates. Areas of potential overlap were produced using the threshold outputs from MAXENT from current bioclim data. In order to evaluate potential historical corridors or overlap between areas for these two species, LIG and LGM distributions were also compared.

2.9. Historical biogeography

Ancestral biogeography was reconstructed following the analytical approach of Voelker et al. (2014) using the R package BioGeoBears (Matzke, 2013a). All distributions were assessed using the species tree produced in BEAST. Seven major biogeographic areas in Africa were defined (Fig. 2, inset): (1) Northern Africa (includes both Sahel and Saharan zones; Linder et al., 2012), (2) West Africa (west of Cross River in eastern Nigeria near border with Cameroon; Penner et al., 2011), (3) Central Africa (core of the continent), including the Gulf of Guinea Islands (Bell et al., 2015; Measey et al., 2007), (4) Albertine Rift (including eastern Democratic Republic of the Congo and western Burundi, Rwanda and Uganda; Linder et al., 2012), (5) East Africa (Kenya, eastern Uganda, eastern Burundi, eastern Rwanda, Tanzania, Malawi, northern Mozambique; Zambia), (6) Horn of Africa (includes Ethiopian and Somali zones; Linder et al., 2012), (7) Southern Africa (south of the Zambezi and Cunene Rivers; Leaché et al., 2014). Madagascar was considered one single biogeographic zone in analyses that included both African and Malagasy lineages and then subdivided into four regions for increased resolution of Malagasy ecosystems (Brown et al., 2014). Dispersal was allowed freely and was not restricted to adjacent areas. Six models of geographic range evolution were compared in a likelihood frame-

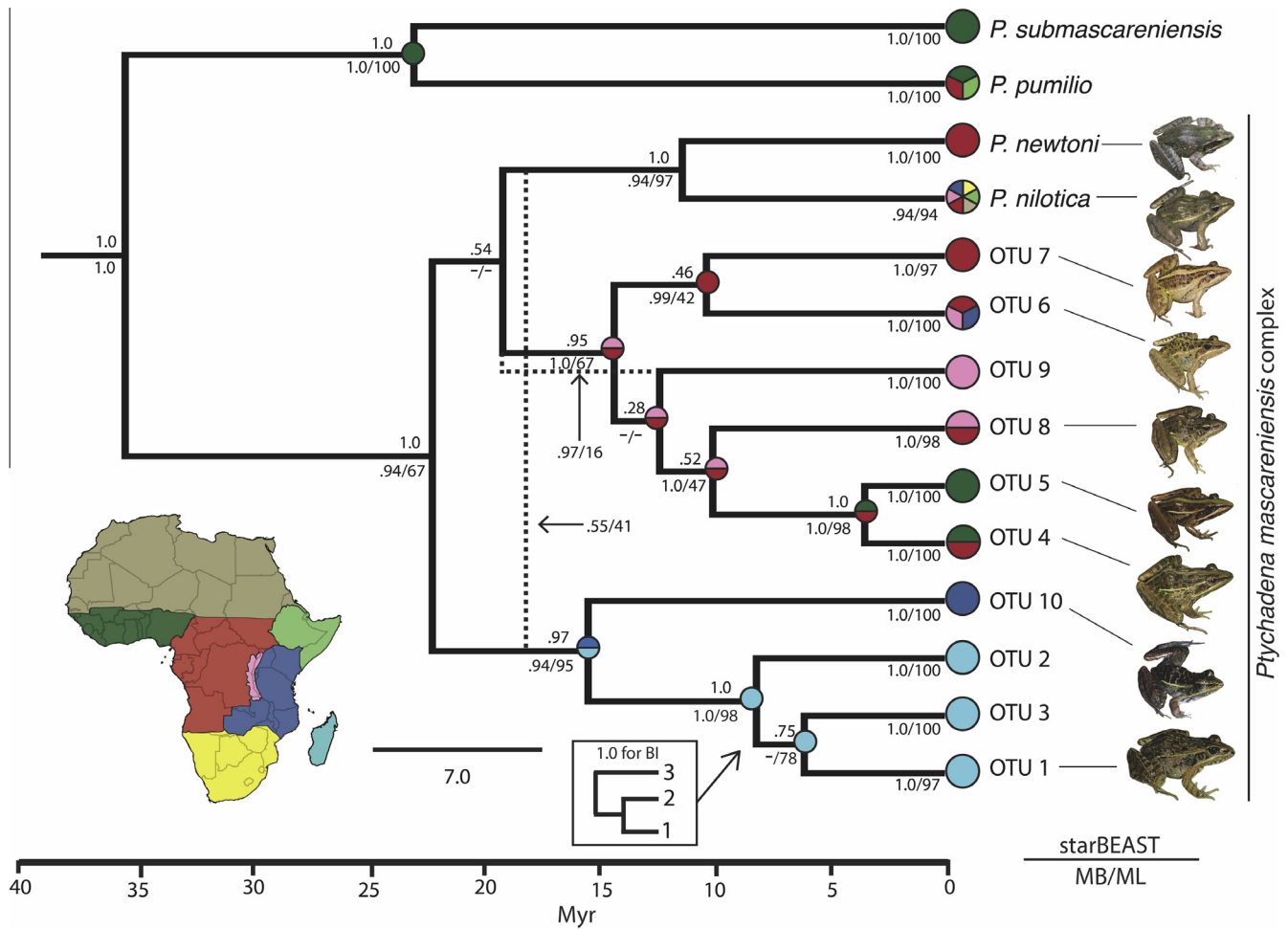


Fig. 2. Species tree reconstructed for phylogenetically identified OTUs using combined DNA data (16S, cytb, RAG1) with the Bayesian Inference of Species Trees (*BEAST; coalescent tree model with a strict molecular clock). Posterior probabilities for branches from the *BEAST analysis are placed above branches. Posterior probabilities for BEAST (mtDNA dataset) and MB (concatenated data) analyses, as well as bootstrap support values for the ML (concatenated data) analyses are placed below branches. Alternative topologies are indicated with dotted lines or within boxes. Lineages are color-coded according to distribution within seven African regions and Madagascar. Ancestral distribution reconstructions using BioGeoBEARS are included at nodes; reconstructions resulting in more than two possible states are not shown. *Ptychadena anchietae* included as additional outgroup but not shown. For interpretation of the references to color in this figure legend, the reader is referred to the web version of this article.

work: (1) Dispersal-Extinction Cladogenesis Model (DEC) similar to Lagrange (Ree and Smith, 2008), which parameterizes dispersal and extinction; (2) DEC + j model (Matzke, 2013b, 2014), which adds long-distance dispersal to the Dispersal-Extinction Cladogenesis (DEC) framework; (3) Dispersal Vicariance Analysis (DIVA) (Ronquist, 1997); (4) Dispersal Vicariance Analysis with long-distance dispersal (DIVA + j) (Matzke, 2013b); (5) Bayesian inference of historical biogeography for discrete areas (BayArea) (Landis et al., 2013); and (6) Bayesian inference of historical biogeography for discrete areas with long-distance dispersal (BayArea) (Matzke, 2013b). Model fit was assessed using the Akaike information criterion (AIC) and likelihood-ratio tests (LRT). The availability of connections between areas (dispersal routes) was unconstrained.

3. Results

3.1. Phylogenetic relationships

Results of three phylogenetic methods (ML using concatenated alignment of three genes, MB using concatenated alignment of three genes, BEAST using mtDNA) were congruent in recovering a

clade that included ten well-supported lineages (OTUs), plus *P. nilotica* (containing the embedded species *P. filwoha*), and *P. newtoni* (Figs. 1–3). *Ptychadena nilotica* and *P. newtoni* were consistently found to be sister species with high support values. A second major clade was reconstructed in all analyses and included three Malagasy lineages (OTUs 1–3) and a single East African lineage (OTU 10). A third clade included six OTUs (4–9) distributed across tropical Africa (western, central, Albertine, and eastern zones), which we herein call the Central African clade. Although the *P. mascareniensis* complex (formerly defined to include all lineages previously identified as *P. mascareniensis*, as well as *P. filwoha*, *P. newtoni* and *P. nilotica*) was consistently found to be monophyletic, the relationship among the three major clades was unstable, and regardless of method, support values were low. BEAST analyses placed the *P. nilotica* and *P. newtoni* clade as the sister group of the Central African clade, while MB and ML results placed the *P. nilotica* and *P. newtoni* clade as the sister group to the Malagasy-East African clade (Figs. 2 and 3). MB analyses of individual mitochondrial markers (16S, cytb) supported the identification of ten OTUs within three major clades. ML analyses reconstructed the same ten OTUs within three major clades, although support values were low for some OTUs (16S: *P. nilotica*; cytb: OTU 1, *P. nilotica*; Fig. S1). The nuclear gene trees from the

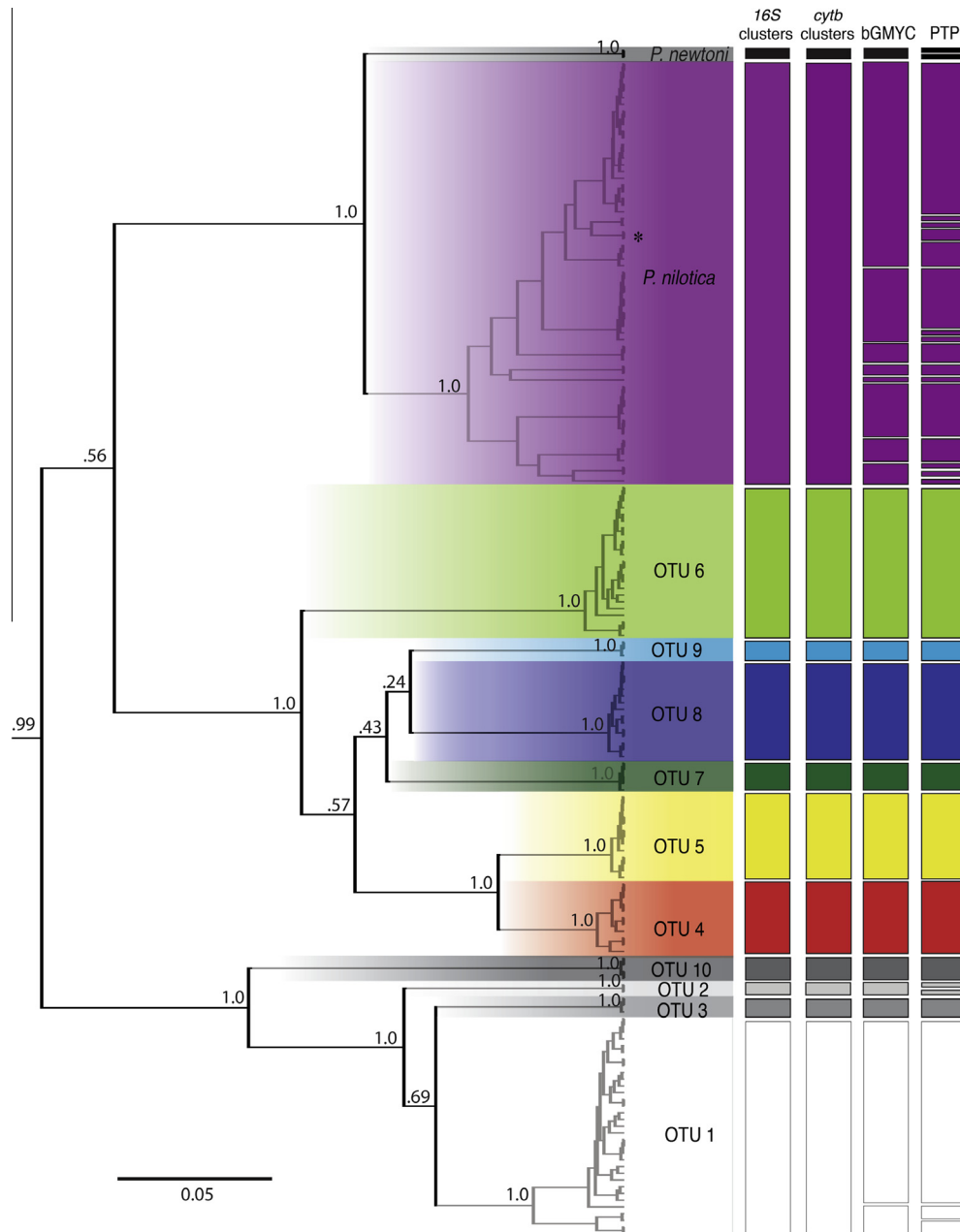


Fig. 3. Results of species-delimitation approaches (clustering algorithms implemented in SpeciesIdentifier, bGMYC and PTP). The full ultrametric tree for frogs of the *Ptychadena mascareniensis* complex, including 177 individuals (excluding outgroup taxa) and 1758 base pairs, using Bayesian inference analysis of the mitochondrial dataset (16S and *cytb*) with BEAST. Recognized OTUs are based on three different methods from left to right: (1) Species Identifier clusters (16S: threshold 2.0–2.5%; *cytb*: threshold 5.5–6.0%); (2) bGMYC (see Fig. S4 for heat map); (3) PTP. Results are color-coded by OTU (OTU 1, white; OTU 2, light grey; OTU 3, medium grey; OTU 4, red; OTU 5, yellow; OTU 6, light green; OTU 7, dark green; OTU 8, dark blue; OTU 9, light blue; OTU 10, dark grey; *P. nilotica* (including *P. filwoha*, indicated by an asterisk), violet; *P. newtoni*, black). For interpretation of the references to color in this figure legend, the reader is referred to the web version of this article.

RAG1 locus exhibited more incomplete lineage sorting than the mitochondrial trees, as expected for nuclear loci compared to mitochondrial loci (Figs. S2 and S3). Mean uncorrected distances of the 16S rRNA and *cytb* genes between the twelve lineages (herein OTUs 1–10, *P. newtoni*, and *P. nilotica*) ranged between 2.85–9.07% and 7.91–22.70%, respectively (Table S5). Intraspecific 16S sequence variation ranged from 0 to 0.64% for all identified lineages, except for *P. nilotica*, which ranged up to 1.55%. Intraspecific *cytb* sequence variation ranged from 0 to 1.63% for all identified lineages, except for OTU 1, which ranged up to 3.05%, and *P. nilotica*, which ranged up to 7.55%.

3.2. Haplotype networks

The relationships among OTUs were also assessed with haplotype networks showing one-step mutations; identical sequences were pooled into a single terminal. Numbers of analyzed sequences and unique haplotypes were as follows ($N_{\text{samples}}/N_{\text{haplotypes}}$): mitochondrial genes 16S (175/61), *cytb* (162/94) and the phased nuclear gene *RAG1* (304/100). Haplotype networks of the mitochondrial 16S rRNA showed a clear separation of haplogroups, which formed distinct and unassociated haplogroups for all 12 lineages (OTUs 1–10, *P. newtoni*, and *P. nilotica*). *Ptychadena nilotica* included three

distinct haplogroups, with the vast majority of haplotypes within one network (AC2087 from Tanzania and AARCG1561, AARCG1562 and AARCG1563 from Mozambique in their own haplogroups; Fig. 4A); *P. filwoha* was included in the largest haplogroup. Haplotype networks of the mitochondrial *cytb* gene also demonstrated distinct networks for all 12 OTUs with additional separation: OTU 1 forming three haplogroups, OTU 3 forming two haplogroups, OTU 6 forming two haplogroups, and *P. nilotica* forming 12 distinct haplogroups, including a single haplogroup for *P. filwoha* (Fig. 4B). The nuclear marker *RAG1* showed little overlap in haplotypes between lineages (Fig. 4C), with shared haplotypes only among OTUs 1 and 2, OTUs 1 and 3, and OTUs 4 and 5, respectively.

3.3. Species delimitation

The number of OTUs identified by ‘clusters’ in SpeciesIdentifier (approach 1, see above) depended on the applied threshold values. The number of recognized clusters increased with decreasing threshold values (Table S6). Threshold values differed between analyzed mitochondrial genes, suggesting different evolutionary rates, with *16S* being slower when compared to the *cytb* gene.

Ranges of 3–17 clusters were identified using *16S* rRNA at thresholds ranging from 1.0% to 5.0% (Fig. 3). At thresholds of 2.0–2.5%, 12 lineages (OTUs 1–10, *P. newtoni*, and *P. nilotica*) were recognized. As thresholds were reduced to 1%, only OTU 1 and *P. nilotica* were split into additional separate clusters. Analyses of *cytb* at a 5.5–6.0% threshold supported all 12 lineages. When thresholds were reduced to 2.0%, again only OTU 1 and *P. nilotica* were additionally subdivided into separate clusters (Table S6).

The bGMYC model (approach 2, see above) and PTP with the best-fit ML search (approach 3, see above) both recovered additional lineages when compared to the SpeciesIdentifier approach (20 lineages identified in bGMYC at the 0.7 threshold, 31 lineages in PTP; Figs. 3 and S4). Most of the additional lineages were identified in OTU 1 and *P. nilotica*; both were subdivided into multiple lineages reflecting geographic structure of the samples. Analyses using bGMYC recovered ten OTUs with confidence; OTU 1 was divided into two lineages, and *P. nilotica* was subdivided into eight lineages, each using approach 2. Analyses using PTP recovered eight OTUs with confidence, including OTUs 3–10 (Fig. 3). OTU 2 and *P. newtoni* were divided into two lineages, and OTU 1 was subdivided into three lineages, each using approach 3. Similar to

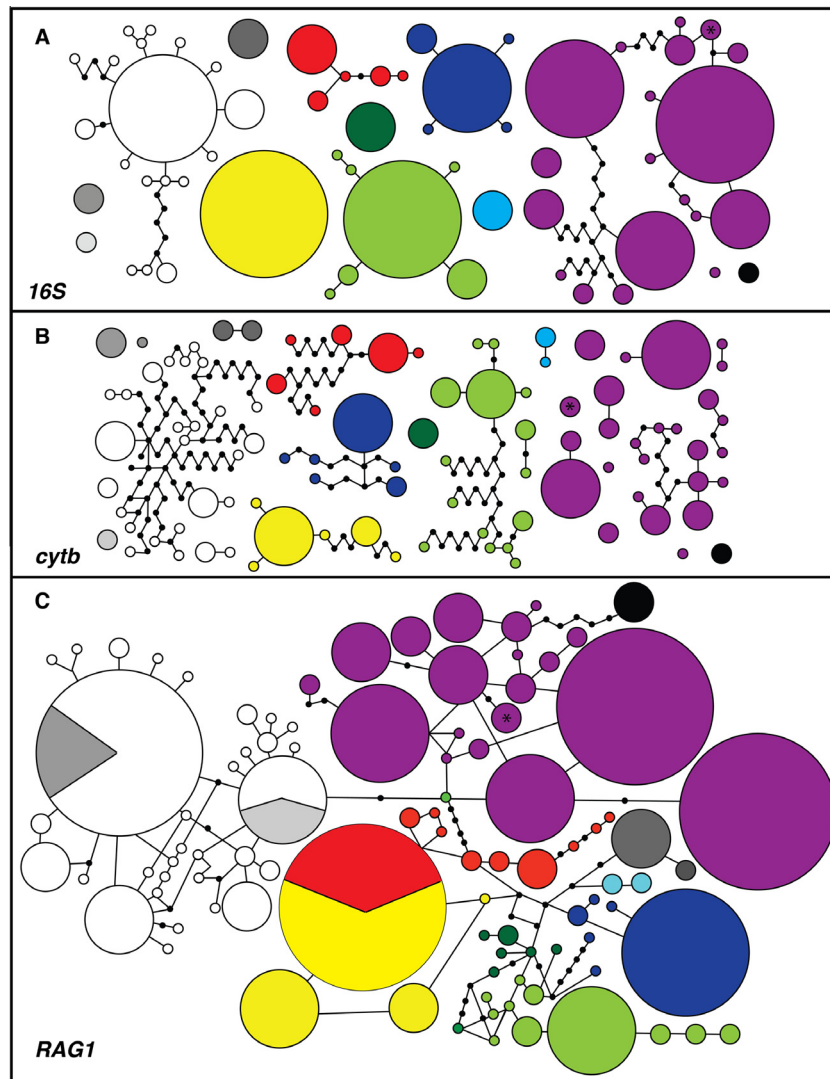


Fig. 4. Relationships among *Ptychadena mascareniensis* complex haplotypes using statistical parsimony networks as implemented in TCS. Each circle in a given network corresponds to one observed haplotype, with the size of each circle proportional to the number of individuals with the observed haplotype. Circles are color-coded by OTU (OTU 1, white; OTU 2, light grey; OTU 3, medium grey; OTU 4, red; OTU 5, yellow; OTU 6, light green; OTU 7, dark green; OTU 8, dark blue; OTU 9, light blue; OTU 10, dark grey; *P. nilotica* (including *P. filwoha*, indicated by an asterisk), violet; *P. newtoni*, black). Small black dots represent hypothetical haplotypes needed to connect the network but not observed among the samples. For interpretation of the references to color in this figure legend, the reader is referred to the web version of this article.

bGMYC, *P. nilotica* was divided into many lineages (16) using PTP. As the automated species delimitation methods achieved similar results but tended to overestimate the number of potential species, we took a conservative approach and used results of clustering analyses to designate species and to reconstruct the species tree and historical biogeography.

3.4. Historical biogeography and divergence dating

Six models of geographic-range evolution were compared in a likelihood framework in BioGeoBEARS for both the entire dataset (Africa + Madagascar), as well as lineages restricted to Madagascar (Table S7). The Dispersal-Extinction Cladogenesis model (DEC) was chosen for both analyses, as it outperformed the other main modeling types (DIVA, BayArea). Though the DEC + J model had a slightly higher likelihood, this more complex model was not a statistically significant improvement over the model without long-distance dispersal, and was thus also excluded from interpretation ($P = 0.12$, $\Delta AIC = 1.24$). Results from ancestral-distribution reconstructions are shown on the *BEAST tree in Fig. 2.

The most recent common ancestor to the *P. mascareniensis* complex (OTUs 1–10, *P. newtoni*, and *P. nilotica*) was dated in the early-Miocene (22.2 Myr, 95% HPD = 15.6–31.0 Myr), diverging into three major clades distributed across mainland Africa, and later dispersing into Madagascar (Fig. 2). A single clade of three lineages within Madagascar (OTUs 1–3) was recovered in all phylogenetic analyses, with its closest sister lineage located in Tanzania (OTU 10). This divergence between OTU 10 and the three Malagasy OTUs is dated within the mid-Miocene (15.5 Myr; 95% HPD = 9.8–22.7 Myr). A second major clade within the *P. mascareniensis* complex (the “Central African clade”) originated 14.3 Myr (95% HPD = 10.0–20.7 Myr) in the mid-Miocene and included six OTUs (4–9) distributed widely across tropical Africa, with its origins in Central Africa or the Albertine Rift (Fig. 2). The

ancestor to the last major clade within the *P. mascareniensis* complex was dated at 11.4 Myr (95% HPD = 6.3–19.2 Myr) and included the widespread *P. nilotica* and its sister species, *P. newtoni*, restricted to the island of São Tomé in the Gulf of Guinea. Without calibration points, confidence intervals on timing of many of the deeper species divergences were rather broad (Fig. S5).

Three lineages were identified within Madagascar (OTUs 1–3), with a most recent common ancestor dated at approximately 8.2 Myr (95% HPD = 9.8–22.7 Myr; Fig. 2) in the late-Miocene. One lineage endemic to Madagascar (OTU 1) was widely distributed and found within all four biogeographic zones (Fig. 5): eastern humid, central highland, western arid, and southwestern sub-arid. Two lineages (OTUs 2, 3) had more limited distributions: OTU 2 was found in the north of Madagascar, as well as on the northeast on the border between the western arid and eastern humid zones. OTU 3 was distributed in two localities on the border between the eastern humid and central highland zones.

The Central Africa Clade (OTUs 4–9) included both range-restricted and broadly distributed species (Figs. 1 and 2). Three of the six OTUs were restricted to a single biogeographic region, with each region being unique (OTU 5, West; OTU 7, Central; OTU 9, Albertine). Two lineages were found within two adjacent Zones: OTUs 4 (Central-West) and OTU 8 (Central-Albertine). OTU 6 was the most widespread lineage, being distributed across three adjacent zones (Central, Albertine, East). A single pair of sister species (OTU 4 and 5) was distributed in West Africa, with OTU 5 exhibiting the farthest distribution west (i.e., Guinea, Côte d'Ivoire, Liberia, Sierra Leone). Only a single lineage within the Central African clade (OTU 6) invaded East Africa.

3.5. Species-distribution modeling

Potential distributions derived from MAXENT SDMs for mainland *Ptychadena* OTUs and species under current climatic conditions

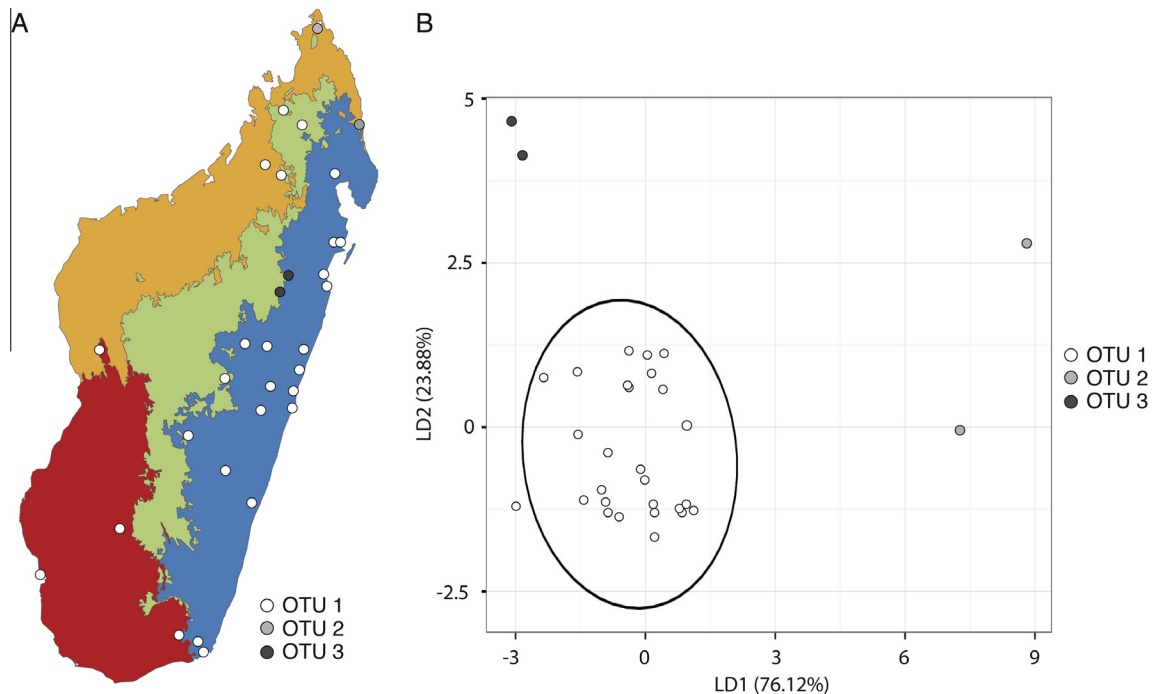


Fig. 5. Species occurrences and Discriminant Function Analysis (DFA) of OTUs present in Madagascar. A. OTUs present in Madagascar with biogeographic areas delimited using the 4-class Generalized Dissimilarity Model (GDM (Brown et al., 2014): eastern humid (blue), central highland/montane (green), western arid (orange), southwestern sub-arid (red) zones. B. DFA of Malagasy lineages (OTUs 1–3). LD1 is most strongly loaded by bio 8 (mean temperature of wettest quarter) and bio10 (mean temperature of warmest quarter) and is meaningful in separating lineages; OTU2 occupies habitats with colder winters when compared to OTU1 and OTU 3. For interpretation of the references to color in this figure legend, the reader is referred to the web version of this article.

are shown in Fig. 6; the SDM for the single Malagasy lineage modeled, OTU 1, is shown in Fig. S6. Last Glacial Maximum (LGM) and Last Interglacial (LIG) distributions are shown in Figs. S7 and S8, respectively. Model performance was ‘very good’ or ‘good’ as indicated by a mean AUC value of 10 model runs (Araújo et al., 2005; Swets, 1988): OTU 1 (0.844), ‘good’; OTU 4 (0.939), ‘very good’; OTU 5 (0.958), ‘very good’; OTU 6 (0.915), ‘very good’; OTU 8 (0.923), ‘very good’; *P. nilotica* (0.886), ‘good’. The ‘minimum training presence logistic threshold’ for each lineage was applied to determine suitable and unsuitable area: OTU 1 (0.1587); OTU 4 (0.4025); OTU 5 (0.3065); OTU 6 (0.2584); OTU 8 (0.3731); *P. nilotica* (0.0791). Under current climatic conditions, known distributions of all *Ptychadena* lineages modeled (OTUs 1, 4, 5, 6, 8, *P. nilotica*) were well explained. An exception was the occurrence of *P. nilotica* in the vicinity of the Nile River within Egypt. In all *Ptychadena*, the potential distributions covered areas larger than the known geographic ranges; partly, these areas were well explained by high suitability in our SDMs (e.g. OTU 8: central Congo basin). However, as this is the nature of potential distribution models (Peterson et al., 2011), areas identified as suitable to frogs exceeded the *a priori* expectable dispersal reach. Sometimes, highly suitable areas were predicted that were isolated and far distant from the known distribution (e.g. OTU 4: West Africa). SDMs showed that the studied *Ptychadena* largely overlapped in climatic dimensions exploited in bioclimatic space (as expressed in their mapped potential distributions). Little overlap and almost mutual exclusion in potential distributions were observed in the closely related OTUs 4 and 5 (Figs. 6A, B and 7A). The opposite was found, i.e. overlap of most suitable potential distributions in the Congo basin (and thus similar bioclimatic dimensions), in the phylogenetically more distant OTUs 6 and 8 (Fig. 6C and D).

Projections into the LGM (Fig. S7) had excellent model fit for most species, and revealed a range of distribution increases and decreases across taxa, mostly accompanied by considerable changes in suitability in the area identified as most suitable under current climate. Potential geographic ranges under current and LGM climate were similar in geographic dimensions only in *P. nilotica*. Overlap between current and LGM distributions of each lineage show that most lineages in this radiation of *Ptychadena* were able to survive in the areas where they are currently recorded or in nearby areas. An exception is OTU 8, where the current area of occupation showed little signal of suitability in the LGM (Fig. S7D).

Compared to the current climate potential distributions, LIG models of all species showed marked decreased geographic ranges (Fig. S8), although fit of these models was much lower. The mapped output suggested refugial stability in the area where they are recorded today (or in adjacent areas) in all *Ptychadena* except in OTU 4 (Fig. S8A), which showed almost complete loss of suitable climatic conditions within its current distribution in coastal Cameroon and Nigeria.

3.6. Bioclimatic niche divergence

Discriminant Function Analysis (DFA) of bioclimatic data of the *P. mascareniensis* complex (OTUs 1–10, *P. newtoni*, and *P. nilotica*) showed numerous African lineages overlapping in niche space, but also identified a number of lineages occupying distinct bioclimatic niches, which were particularly tied to differences in temperature (Fig. 6F). All Malagasy OTUs (1, 2, 3) and OTU 5 were separated from all other species on LD1 (primary Linear Discriminant axis of variance), which is influenced by maximum temperature of warmest period and mean temperature of driest and coldest quarters. OTU 5 occupied a distinct habitat from all other African species, reflecting the cooler temperatures and altitudinal range of this lineage in the Guinea Highlands. The LD2 axis was primarily influenced by mean temperature of warmest quarter separating

OTU 5 and *P. nilotica* from the rest. Principal Component Analyses (PCA) of bioclimatic data of the *P. mascareniensis* complex also were highly influenced by temperature, although distinctions between species were less pronounced than in DFA, as expected when broadly distributed species are combined with limited-distribution species in analyses (Figs. S4 and S9A). The large variability in climatic conditions across the distribution of *P. nilotica* appears to encompass all of the environmental conditions for all other lineages (Fig. S9A).

As all of the Malagasy lineages were distinct from their sister clades on continental Africa in DFA (highlighting that conditions on Madagascar are different from those found within the rest of the African continent), separate analyses restricted to this radiation (OTUs 1–3) were done. OTU 1 had a much broader geographic range compared to OTUs 2 and 3 as demonstrated by its presence within all four biogeographic regions of Madagascar (Fig. 5A), and also appears to occupy a broader bioclimatic space in PCA analyses (Fig. S9B). In the DFA, LD1 explained most (76.12%) of the variation, and was influenced by mean temperature of wettest quarter and mean temperature of warmest quarter, indicating that OTU 2 occupies habitats with colder winters when compared to OTUs 1 and 3 (Fig. 5B). LD2 was mostly influenced by annual mean temperature and mean temperature of warmest quarter, separating OTU 3 from OTU 1 and OTU 2, but only explained 23.9% of the variation.

For analyses restricted to the Central African clade (OTUs 4–9), LD1 for DFA was most heavily loaded with isothermality, whereas LD2 was loaded with mean temperature of warmest quarter. OTUs 6, 7 and 8 formed one overlapping grouping in the DFA (Fig. 7B). In contrast, OTUs 4, 5, and 9 all occupied unique habitat space in both DFA and PCA analyses (Fig. S9A and C). As seen in the larger phylogenetic analysis (Fig. 6F), OTU 5 experienced a stronger seasonality, OTU 4 was present in stable warmer habitats, and OTU 9 was found in stable cooler habitats.

The bioclimatic envelopes of OTUs 4 and 5 were significantly different, with current areas of potential overlap east of the current ranges of either lineage in the Congo basin, and no overlapping areas within their realized distributions in West Africa (Fig. 7). Bioclimatic niche identity between the two lineages had values of I: 0.736 and D: 0.465, while comparisons to random background points were I: 0.9069, D: 0.6427 (OTU 4 mapped onto a background of OTU 5) and I: 0.85, D: 0.567 (OTU 5 mapped onto a background of OTU 4), with $p < 0.001$ for each. For each of the occupied areas of their distribution, OTU 4 and OTU 5 had adjacent areas of potential habitat, although in each case the neighboring region was unoccupied (Fig. 7A). LGM estimates of these lineages showed a corridor of suitable habitat along coastal West Africa for OTU 5, whereas no corridor was present in the LGM for OTU 4 to reach its most western predicted suitable habitat in Liberia and Sierra Leone (Fig. 7C and D).

4. Discussion

4.1. Cryptic species diversity

Based on an integrative evaluation of the available results, we are convinced that the *P. mascareniensis* complex contains a substantial amount of undescribed species diversity. We identify ten OTUs and confirm the validity of two previously described species, *P. nilotica* and *P. newtoni*, within this complex. Four of the OTUs identified herein are recognized for the first time, while additional genetic evidence upholds the identification of six lineages recognized previously (Dehling and Sinsch, 2013; Vences et al., 2004). We propose that seven candidate species occur in Africa (See Fig. 1 for map of occurrences and Table S8 for descriptions of distributions of lineages). Some OTUs may correspond with species

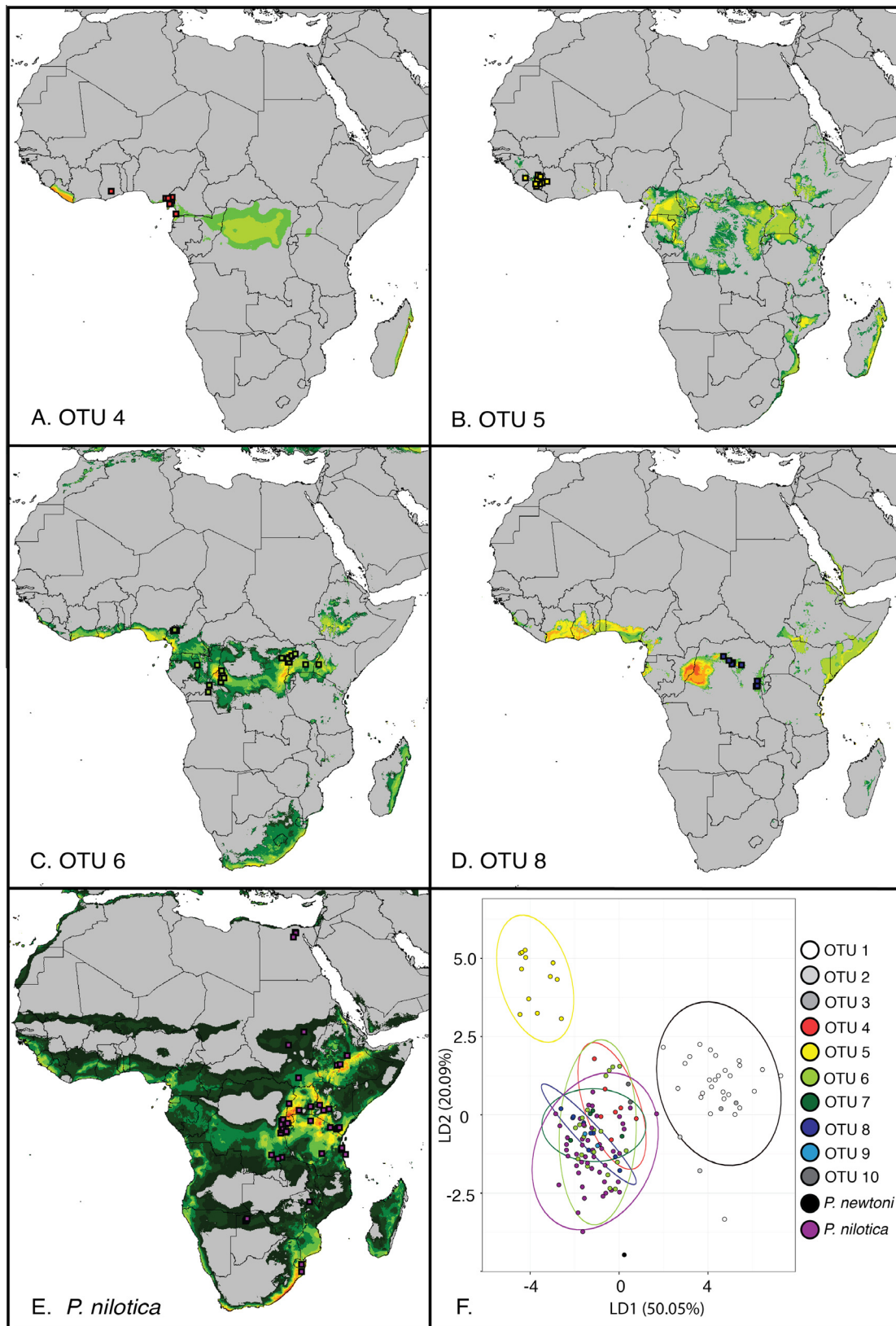


Fig. 6. Species Distribution Modeling (SDM) and Discriminant Function Analysis (DFA) of lineages within the *Ptychadena mascareniensis* complex. Potential distributions for (A) OTU 4, (B) OTU 5, (C) OTU 6, (D) OTU 8, and (E) *P. nilotica* (including *P. filwoha*) constructed under current climatic conditions using genetically confirmed records (light blue boxes) and based on MAXENT SDM with six bioclim variables (bio1, 5, 6, 12, 13, 14) per lineage. Warmer colors advocate higher suitability (i.e. high values under MAXENT's logistic output, ranging 0–1). Grey suggests unsuitable area, when applying the 'minimum training presence logistic threshold' for each lineage (provided in Section 3). (F) DFA of *P. mascareniensis* complex with LD1 most heavily loaded with bio8 (mean temperature of wettest quarter) and LD2 most heavily loaded by bio10 (mean temperature of warmest quarter). OTU 1 (Madagascar) and OTU 5 occupy a habitat distinct from all other species. Ellipses are the same color as the points for their respective lineage, except for OTU 1 (white), which is outlined in black. For interpretation of the references to color in this figure legend, the reader is referred to the web version of this article.

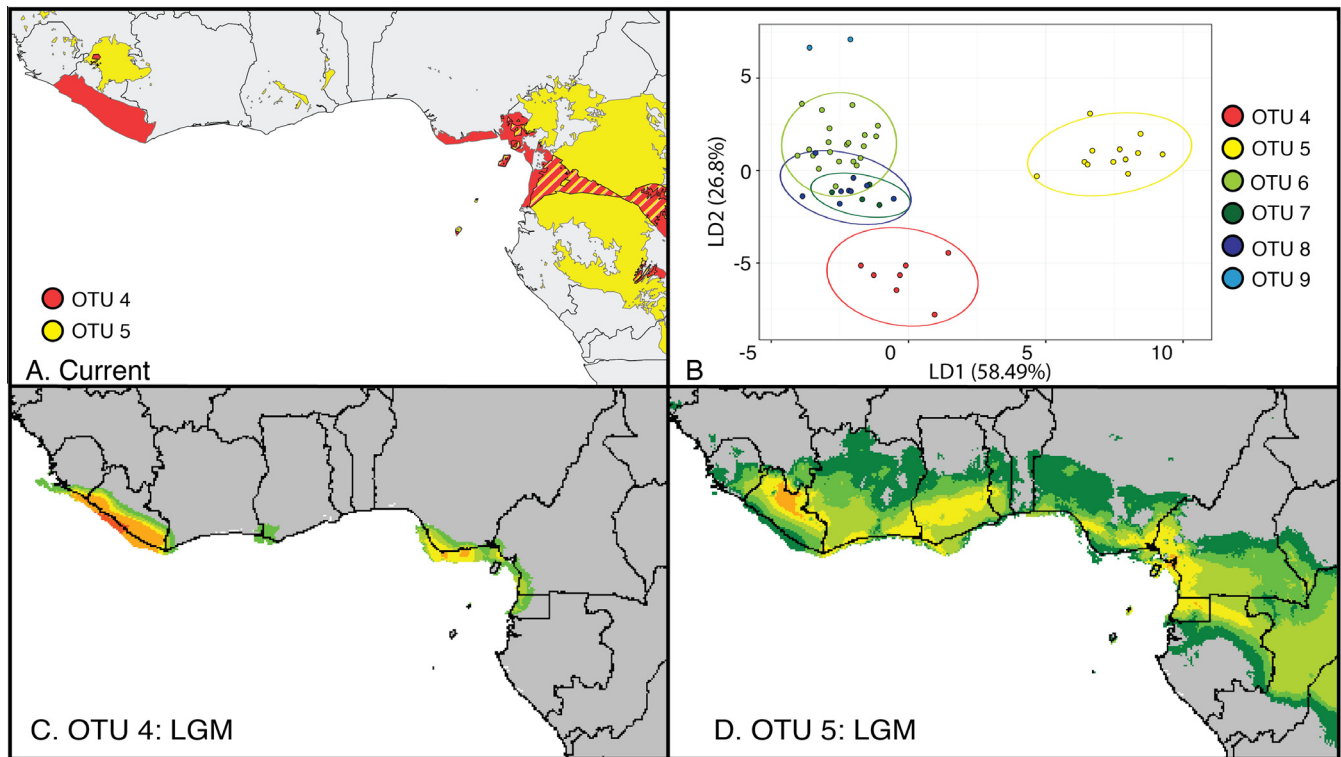


Fig. 7. Significantly differing bioclimatic niches of OTU 4 and OTU 5 through time. (A) Species-distribution models of OTU 4 (red) and OTU 5 (yellow) during current climatic scenario with overlap shown striped; current areas of potential overlap are east of the current range of either species in the Congo basin with no overlapping areas within their realized distributions in West Africa. (B) Discriminant Function Analysis (DFA) of Central African clade (OTUs 4–9), demonstrating clear separation of OTU 4 and OTU 5 from the other four lineages. LD1 is most heavily loaded with bio3 (isothermality), and LD2 is loaded with bio10 (mean temperature of warmest quarter). (C–D) Species Distribution Models of OTUs 4 and 5 during Last Glacial Maximum constructed using genetically confirmed records and based on MAXENT SDM with six bioclim variables (bio1, 5, 6, 12, 13, 14) per lineage. Warmer colors advocate higher suitability (i.e. high values under MAXENT's logistic output, ranging 0–1). Grey suggests unsuitable area, when applying the 'minimum training presence logistic threshold' for each lineage (provided in Section 3). Westward expansion of OTU 5 to Liberia and Sierra Leone may have occurred during the LGM via the corridor of suitable habitat along coastal West Africa; no suitable corridor existed for OTU 4, despite suitable habitat for OTU 4 in Liberia. For interpretation of the references to color in this figure, the reader is referred to the web version of this article.

previously synonymized with *P. mascareniensis*; therefore, morphological comparison of candidate species and original type material is needed.

The identification of undescribed species diversity is based on the concordance among species-delimitation methods, but also on visual inspection of the haplotype networks that demonstrate concordant differentiation of mtDNA vs. *RAG1* (Fig. 4). In two instances, nuclear haplotypes are shared among OTUs: OTUs 4 and 5 share their most common *RAG1* haplotype, and the three Malagasy OTUs (1, 2 and 3) also share haplotypes of this gene. In these two cases, the identity of the respective OTUs as independently evolving entities, (i.e., species) is questionable and requires confirmation from additional lines of evidence. OTUs 4 and 5 were identified as independent lineages using all species delimitation methods and showed mutual exclusion in their potential distributions (Figs. 3 and 7); hence, we retain them as separate lineages until further study can be completed. In the case of the Malagasy lineages, OTUs 2 and 3 occupy small, possibly relictual ranges and are in direct geographical contact with the widespread lineage 1. The absence of differentiation in the *RAG1* gene might suggest extensive hybridization and admixture and a status of deep conspecific lineages, but more information on the morphology, bioacoustics, and hybrid zones of these lineages is needed to ascertain their status. Until these additional studies are completed, we suggest that all three Malagasy lineages be identified as *P. mascareniensis*.

Our decision to retain *P. nilotica* and the widespread Malagasy lineage as single species was conservative given results of automated species-delimitation methods based on branch-length

dynamics (i.e., bGMYC, PTP), which estimated many more lineages when compared to methods that cluster sequences based on pairwise distances (i.e., SpeciesIdentifier). In addition, given that 16S, *cytb* and *RAG1* sequences of *P. filwoha* are embedded within *P. nilotica*, we treat them as a single taxon but recommend future taxonomic studies, including morphological analysis of type specimens. Previous analyses of morphology revealed only subtle differences between these two species, including size (*P. filwoha*: males 26–34 mm, females 30–40 mm; *P. nilotica*: males 34–47, females 37–58) and pattern on the posterior face of the thigh (Largen, 1997).

4.2. Historical biogeography and divergence dating

Dating estimates suggest that the most recent common ancestor of the *P. mascareniensis* complex likely arose in the early Miocene, approximately 22.2 Myr ago. As with all timetrees based on secondary calibrations (Graur and Martin, 2004) or rate calibrations derived from distant taxa, we emphasize that divergence estimates include a large amount of uncertainty. Regardless, it seems clear that most divergences within the *P. mascareniensis* complex occurred in Miocene-Pliocene times, before the onset of the Pleistocene climatic oscillations. In these periods, lowland rainforest moved southward with the equatorial shift, and high-altitude areas arose by continental uplift (Lovett, 1993). The divergence between those candidate species distributed in West Africa (OTUs 4, 5) was estimated to be in the Pliocene with confidence intervals that include the Pleistocene, which suggests that climate during these more recent epochs may have influenced current pat-

terns of distribution. A pattern of relatively young species within West Africa has also been reconstructed in a number of vertebrate groups, including *Arthroleptis*, *Silurana*, and *Xenopus* frogs (Blackburn, 2008; Evans et al., 2004) and lizards of the *Agama agama* complex (Leaché et al., 2014).

Central Africa, including the central biogeographic zone and the montane Albertine Rift, is a cradle of diversity for the *P. mascareniensis* clade, with the ancestor of at least one major clade originating here in the mid-Miocene before dispersing east and west. Central Africa has been a center of diversification in other amphibian lineages, with the most recent common ancestors of both *Arthroleptis* and *Silurana* reconstructed in Central Africa (Blackburn, 2008; Evans et al., 2004). Central Africa was also found to be a diversity hotspot for African clawed frogs of the genus *Xenopus*, with over half of the known species, including six recently described and one resurrected, occurring in this region (Evans et al., 2015).

Out-of-Africa overseas dispersal has occurred twice within the *P. mascareniensis* complex to islands off both the west and east coasts. *Ptychadena newtoni* from the island of São Tomé appears to have split from its mainland sister species, *P. nilotica*, much earlier than the Pleistocene, supporting the previously proposed hypothesis that this population reached the island naturally and was not introduced by humans (Measey et al., 2007). The monophyletic grouping of Malagasy lineages and identification of its sister lineage from Tanzania (OTU 10) provides evidence that a single colonization of Madagascar occurred from an East African population. Although fossil *P. mascareniensis* from Madagascar are currently known only from Pleistocene sites (Burney et al., 2008), preliminary estimates of divergence times from mainland African lineages are much older according to the present study (15.5 Myr) and to Crottini et al. (2012), who obtained pre-Pliocene estimates between 8 and 13 Myr (CIs 2–24 Myr).

4.3. Bioclimatic niche

The bioclimatic envelopes were remarkably well conserved within the African *Ptychadena* radiation, with most lineages distributed in areas of similar temperature and rainfall conditions and exhibiting low niche divergence. One exception to this conservation in bioclimatic niche was a lineage exclusively distributed in West Africa (OTU 5) within Côte d'Ivoire, Guinea, Liberia, and Sierra Leone. This lineage occupies a distinct habitat at slightly higher elevations within a more temperate region. The examination of the range of its sister lineage (OTU 4), the only other known lineage present in West Africa, showed mutual exclusion in their potential distributions, and a niche-identity test confirmed that they occupied different climatic space in adjacent highland and lowland localities. Within West Africa, OTU 4 was modeled to occur in coastal regions of Liberia and Sierra Leone, but is recorded only as far west as Ghana. Likewise, OTU 5 was modeled to occur more widely in Central Africa, but is not known there. Dry climate-cycle estimates (LGM model) for OTU 5 revealed a wide corridor of suitable habitat along coastal West Africa, with a small region of acceptable habitat in coastal Benin for dispersal through the Dahomey Gap, which may have allowed westward expansion from a shared ancestor in Central Africa. In contrast, dry climate (LGM) estimates of OTU 4 show a range that is almost identical to contemporary recorded localities within coastal Cameroon and Nigeria, as well as an isolated Ghanaian population. No corridor of suitable habitat was present in the dry climate model to allow OTU 4 to disperse through Liberia to reach its most western predicted suitable habitat within Liberia and Sierra Leone. Its presence in Ghana, however, does suggest that some range expansion occurred.

Estimations of suitable climatic conditions, and thus areas of potentially suitable habitat, were a good match for known distributions for almost all *Ptychadena* lineages. *Ptychadena nilotica*, however, occurs in the Nile Delta of Egypt, yet these regions have no areas of suitable habitat predicted. As all molecular loci placed the Egyptian specimens within a clade of East African *P. nilotica*, these do not appear to be cases of mistaken identity or unrecognized diversity. For the Ethiopian region, this species is more widespread along the Nile than is currently documented, and the lack of additional locality samples in this divergent habitat type influences the model to under-predict in this region. Conversely, *P. nilotica* may exist only in isolated microhabitats along the shore; thus, the coarse ca. 1 km grid of environmental factors may miss these small pockets of landscape. Increased sampling may also reveal new localities that will contribute not only genetic but spatial clarity to the extent and distribution of this lineage in these areas.

The Malagasy lineages were found to occupy a different bioclimatic niche when compared to the African lineages, though this result is apparent only in DFA due to the very broad environmental range that *P. nilotica* occupies. Due to the physical distance between Madagascar and mainland Africa, as well as the potential for spatial autocorrelation due to the divergent climate of Madagascar compared with mainland Africa, it is difficult to determine if a niche shift has actually occurred for these lineages. Despite the distinct space in DFA plots, we suspect that a bioclimatic niche shift has not occurred, as OTU 1 is found across a very wide variety of habitats in Madagascar from lowland areas to the tops of mountains.

Partitioning within Madagascar based on biozones was greater than expected, with the greatest number of populations present in the eastern humid zone, which is influenced by trade winds from the Indian Ocean, causing an increase in moisture on the eastern slopes of the island. The potential distribution of the widely distributed lineage, OTU 1, shows that this species has a much broader environmental tolerance when compared to the two other Malagasy lineages. Unfortunately, the role of bioclimatic niche in demarcating these three lineages could not be determined given the restricted distributions of OTU 2 and OTU 3, as well as lack of phylogenetic resolution in the relationships among the three Malagasy lineages. With current sampling levels, it is unclear whether these are three separate species, or three lineages within the same species that are expanding from separate small refugial distributions, as has been observed in other Malagasy taxa including the geckos *Uroplatus allaudi* and *U. pietschmanni* (Raxworthy et al., 2008). Ancestral distributions of mtDNA clades of the arid-adapted Malagasy bullfrog, *Laliostoma labrosum*, also suggest potential refugia in northern Madagascar (Pabijan et al., 2015).

5. Conclusions

This study represents the most comprehensive genetic investigation of a Pan-African amphibian species group (with the exception of Furman et al. (2015)) and provides an important benchmark for future studies of widespread African anuran lineages. Species delimitation provided evidence of hidden diversity, with 10 lineages identified within nominal *P. mascareniensis*, seven distributed across mainland Africa, and three on Madagascar. Based on the results of an evaluation of various species-delimitation procedures, we consider the *P. mascareniensis* complex to contain: *P. nilotica* (including *P. filwoha*), *P. newtoni*, *P. mascareniensis* sensu stricto (containing the three Malagasy lineages; OTUs 1–3), and seven candidate species currently named *P. cf. mascareniensis* (OTUs 4–10) occurring in Africa. Candidate species distributed in West Africa (OTU 4, 5) require closer examination as a result of more recent diversification estimates and shared RAG-1

haplotypes. Central Africa and the Albertine Rift are identified as a hotspot of diversity with diversification having occurred throughout the Miocene and Pliocene. The combination of phylogenetic analysis and species distribution modeling revealed the Congo basin to be a hotspot of speciation within this group, and showed a consistent pattern of niche conservation coupled with range expansion. We have demonstrated the utility in combining phylogenetic and ecological data to reconstruct the biogeography of a widespread and notoriously difficult species complex, and we advocate that future studies use these methods as an objective means to assess biogeographic patterns in other taxa.

Author contributions

This collaboration stems from shared interests among co-authors in the population differentiation and systematics of African frogs. B.M.Z. conceived the study with the help of S.L. B.M.Z. and L. P.L. completed phylogenetic reconstructions and species delimitation analyses with advice from M.F.B., M.P. and M.V. S.L. completed species distribution modeling, and L.P.L. analyzed niche divergence and historical niche. B.M.Z. drafted the manuscript with assistance from L.P.L. and S.L. All authors contributed either genetic samples or molecular data (see acknowledgements for research facilities) from collected frogs for analysis, and reviewed and approved the final manuscript.

Acknowledgements

Many thanks to W. Böhme (ZFMK, Bonn), R. Drewes and J. Vin-dum (CAS, San Francisco), J. McGuire and C. Spencer (MVZ, Berkeley), D. Modrý (University of Veterinary and Pharmaceutical Sciences, Brno), and J. Rosado (MCZ, Harvard) who made specimens under their care available and/or donated tissues for this study. An Ethel K. Allen, Sigma Delta Epsilon-Graduate Women in Science Fellowship and a Robert G. Goellet research award from the Museum of Comparative Zoology to B.M.Z. funded this work. A Putnam Expedition Grant from the Museum of Comparative Zoology supported fieldwork by B.M.Z. in Ethiopia; B.M.Z. thanks T. Hailu (Ethiopian Wildlife Conservation Department) for permit assistance, R. Kerney and D. Pawlos for accompaniment in the field, and J. Hanken for laboratory space and mentorship. Fieldwork by E.G. in DRC was funded by the Percy Sladen Memorial Fund, an IUCN/SSC Amphibian Specialist Group Seed Grant, K. Reed, M.D., research funds from the Department of Biology at Villanova University, a National Geographic Research and Exploration Grant (no. 8556-08), University of Texas at El Paso, and the National Science Foundation (DEB-1145459); E.G. and C.K. thank their field companions D. Hughes, M. Aristote, W. Moninga, J.-P. Mokanse, M. Zigabe, A. Marcel, M. Luhumyo, J. and F. Akuku, F. Alonda and the late A. M'Mema. Permits to work in the Democratic Republic of Congo were facilitated by the Centre de Recherche en Sciences Naturelles and the Institut Congolais pour la Conservation de la Nature. We acknowledge A. Betancourt of the UTEP BBRC Genomic Analysis Core Facility, which is supported by grants from the National Center for Research Resources (5G12RR008124-12) and the National Institute on Minority Health and Health Disparities (8G12MD007592-12) from the National Institutes of Health, for services and facilities provided. Fieldwork by ZTN in the Democratic Republic of Congo was supported by the Belgian National Focal Point to the Global Taxonomy Initiative. C.D.B. thanks The Centre for African Studies Basel, Humer-Stiftung zur Förderung des wissenschaftlichen Nachwuchses, Freiwillige Akademische Gesellschaft Basel for support and funding. Fieldwork in Tanzania by C.D.B. was conducted with COSTECH permit No. 2013-341-NA-2013-121. V.G. was supported by the Czech Science Foundation

(GACR, project number 15-13415Y), and Ministry of Culture of the Czech Republic (DKRVO 2016/15, National Museum, 00023272). M. V. and M.P. thank the Volkswagen Foundation, Deutsche Forschungsgemeinschaft and Humboldt Foundation for supporting their research in Madagascar, and the Malagasy authorities for research and export permits. We extend thanks to R. Drewes for use of the photograph of *Ptychadena newtoni*.

Appendix A. Supplementary material

Supplementary data associated with this article can be found, in the online version, at <http://dx.doi.org/10.1016/j.ympev.2016.09.018>.

References

- Abascal, F., Zardoya, R., Telford, M.J., 2010. TranslatorX: multiple alignment of nucleotide sequences guided by amino acid translations. *Nucleic Acids Res.* 38, W7–W13.
- Ahmadzadeh, F., Flecks, M., Carretero, M.A., Böhme, W., Ihlow, F., Kapli, P., Miraldo, A., Rödder, D., in press. Separate histories in both sides of the Mediterranean: phylogeny and niche evolution of ocellated lizards. *J. Biogeogr.* 43, 1242–1253.
- Araújo, M.B., Pearson, R.G., Thuiller, W., Erhard, M., 2005. Validation of species-climate impact models under climate change. *Glob. Change Biol.* 11, 1504–1513.
- Beaumont, L.J., Hughes, L., Poulsen, M., 2005. Predicting species distributions: use of climatic parameters in BIOCLIM and its impact on predictions of species' current and future distributions. *Ecol. Model.* 186, 251–270.
- Bell, R.C., Drewes, R.C., Channing, A., Gvoždík, V., Kielgast, J., Lötters, S., Stuart, B.L., Zamudio, K.R., 2015. Overseas dispersal of *Hyperolius* reed frogs from Central Africa to the oceanic islands of São Tomé and Príncipe. *J. Biogeogr.* 42, 65–75.
- Blackburn, D.C., 2008. Biogeography and evolution of body size and life history of African frogs: phylogeny of squeakers (*Arthroleptis*) and long-fingered frogs (*Cardioglossa*) estimated from mitochondrial data. *Mol. Phylogenet. Evol.* 49, 806–826.
- Blair, C., Noonan, B.P., Brown, J.L., Raselimanana, A.P., Vences, M., Yoder, A.D., 2015. Multilocus phylogenetic and geospatial analyses illuminate diversification patterns and the biogeographic history of Malagasy endemic plated lizards (Gerrhosauridae: Zonosaurinae). *J. Evol. Biol.* 28, 481–492.
- Blaxter, M., Mann, J., Chapman, T., Thomas, F., Whitton, C., Floyd, R., Abebe, E., 2005. Defining operational taxonomic units using DNA barcode data. *Philos. Trans. R. Soc. Lond. Ser. B, Biol. Sci.* 360, 1935–1943.
- Booth, T.H., Nix, H.A., Busby, J.R., Hutchinson, M.F., 2014. Bioclim: the first species distribution modelling package, its early applications and relevance to most current MaxEnt studies. *Divers. Distrib.* 20, 1–9.
- Brown, J.L., Cameron, A., Yoder, A.D., Vences, M., 2014. A necessarily complex model to explain the biogeography of the amphibians and reptiles of Madagascar. *Nat. Commun.* 5, e5046.
- Burney, D.A., Vasey, N., Godfrey, L.R., Ramilisonina, Jungers, W.L., Ramarolahy, M., Raharivony, L., 2008. New findings at Andrahomana Cave, southeastern Madagascar. *J. Cave Karst Stud.* 70, 13–24.
- Busby, J.R., 1991. BIOCLIM – a bioclimate analysis and prediction system. *Plant Prot. Q.* 6, 8–9.
- Chan, L.M., Brown, J.L., Yoder, A.D., 2011. Integrating statistical genetic and geospatial methods brings new power to phylogeography. *Mol. Phylogenet. Evol.* 59, 523–537.
- Clement, M., Posada, D., Crandall, K.A., 2000. TCS: a computer program to estimate gene genealogies. *Mol. Ecol.* 9, 1657–1659.
- Crottini, A., Madsen, O., Poux, C., Strauss, A., Vieites, D.R., Vences, M., 2012. Vertebrate time-tree elucidates the biogeographic pattern of a major biotic change around the K-T boundary in Madagascar. *Proc. Natl. Acad. Sci. USA* 109, 5358–5363.
- Dehling, J.M., Sinsch, U., 2013. Diversity of Ridged Frogs (Anura: Ptychadenidae: *Ptychadena* spp.) in wetlands of the upper Nile in Rwanda: morphological, bioacoustic, and molecular evidence. *Zool. Anzeiger* 253, 143–157.
- Dowell, S.A., Hekkala, E.R., 2016. Divergent lineages and conserved niches: using ecological niche modeling to examine the evolutionary patterns of the Nile monitor (*Varanus niloticus*). *Evol. Ecol.* 30, 471–475.
- Elith, J., Graham, C.H., Anderson, R.P., Dudík, M., Ferrier, S., Guisan, A., Hijmans, R.J., Huettmann, F., Leathwick, J.R., Lehmann, A., Li, J., Lohmann, L.G., Loiselle, B.A., Manion, G., Moritz, C., Nakamura, M., Nakazawa, Y., Overton, J. McC. M., Townsend Peterson, A., Phillips, S.J., Richardson, K., Scachetti-Pereira, R., Schapire, R.E., Soberón, J., Williams, S., Wisz, M.S., Zimmermann, N.E., 2006. Novel methods improve prediction of species' distributions from occurrence data. *Ecography* 29, 129–151.
- Elith, J., Phillips, S.J., Hastie, T., Dudík, M., Chee, Y.E., Yates, C.J., 2011. A statistical explanation of MaxEnt for ecologists. *Divers. Distrib.* 17, 43–57.
- Evans, B.J., Carter, T.F., Greenbaum, E., Gvoždík, V., Kelley, D.B., McLaughlin, P.J., Pauwels, O.S.G., Portik, D.M., Stanley, E.L., Tinsley, R.C., Tobias, M.L., Blackburn,

- D.C., 2015. Genetics, morphology, advertisement calls, and historical records distinguish six new polyploid species of African clawed frog (*Xenopus*, Pipidae) from West and Central Africa. *PLoS ONE* 10, e0142823.
- Evans, B.J., Kelley, D.B., Tinsley, R.C., Melnick, D.J., Cannatella, D.C., 2004. A mitochondrial DNA phylogeny of African clawed frogs: phylogeography and implications for polyploid evolution. *Mol. Phylogenet. Evol.* 33, 197–213.
- Evans, B.J., McGuire, J.A., Brown, R.M., Andayani, N., Supriatna, J., 2008. A coalescent framework for comparing alternative models of population structure with genetic data: evolution of Celebes toads. *Biol. Lett.* 4, 430–433.
- Ficetola, G.F., Thuiller, W., Maud, C., 2007. Prediction and validation of the potential global distribution of a problematic alien invasive species—the American bullfrog. *Divers. Distrib.* 13, 476–485.
- Frost, D., 2016. *Amphibian Species of the World: An Online Reference*. Version 6.0 (1 January 2016). American Museum of Natural History, New York, USA.
- Fujisawa, T., Barraclough, T.G., 2013. Eliminating species using single-locus data and the Generalized Mixed Yule Coalescent approach: a revised method and evaluation on simulated data sets. *Syst. Biol.* 62, 707–724.
- Furman, B.L.S., Bewick, A.J., Harrison, T.L., Greenbaum, E., Gvoždík, V., Kusamba, C., Evans, B.J., 2015. Pan-African phylogeography of a model organism, the African clawed frog *Xenopus laevis*. *Mol. Ecol.* 24, 909–925.
- Graur, D., Martin, W., 2004. Reading the entrails of chickens: molecular timescales of evolution and the illusion of precision. *Trends Genet.* 20, 80–86.
- Guillaumet, A., Crochet, P.-A., Pons, J.-M., 2008. Climate-driven diversification in two widespread *Galerida* larks. *BMC Evol. Biol.* 8, 32.
- Heikkinen, R.K., Luoto, M., Araújo, M.B., Virkkala, R., Thuiller, W., Sykes, M.T., 2006. Methods and uncertainties in bioclimatic envelope modelling under climate change. *Prog. Phys. Geogr.* 30, 751–777.
- Heled, J., Drummond, A.J., 2010. Bayesian inference of species trees from multilocus data. *Mol. Biol. Evol.* 27, 570–580.
- Hernandez, P.A., Graham, C.H., Master, L.L., Albert, D.L., 2006. The effect of sample size and species characteristics on performance of different species distribution modeling methods. *Ecography* 29, 773–785.
- Hijmans, R.J., Cameron, S.E., Parra, J.L., Jones, P.G., Jarvis, A., 2005. Very high resolution interpolated climate surfaces for global land areas. *Int. J. Climatol.* 25, 1965–1978.
- Hillis, D.M., Bull, J.J., 1993. An empirical test of bootstrapping as a method for assessing confidence in phylogenetic analysis. *Syst. Biol.* 42, 182–192.
- Landis, M.J., Matzke, N.J., Moore, B.R., Huelsenbeck, J.P., 2013. Bayesian analysis of biogeography when the number of areas is large. *Syst. Biol.* 62, 789–804.
- Lanfear, R., Calcott, B., Ho, S.Y., Guindon, S., 2012. Partitionfinder: combined selection of partitioning schemes and substitution models for phylogenetic analyses. *Mol. Biol. Evol.* 29, 1695–1701.
- Largen, M.J., 1997. Two new species of *Ptychadena* Boulenger, 1917 (Amphibia, Anura, Ranidae) from Ethiopia, with observations on other members of the genus recorded from this country and a tentative key for their identification. *Trop. Zool.* 10, 223–246.
- Leaché, A.D., Wagner, P., Linkem, C.W., Böhme, W., Papenfuss, T.J., Chong, R.A., Lavin, B.R., Bauer, A.M., Nielsen, S.V., Greenbaum, E., Rödel, M.-O., Schmitz, A., LeBreton, M., Ineich, I., Chirio, L., Ofori-Boateng, C., Eniang, E.A., Baha El Din, S., Lemmon, A.R., Burbrink, F.T., 2014. A hybrid phylogenetic–phylogenomic approach for species tree estimation in African *Agama* lizards with applications to biogeography, character evolution, and diversification. *Mol. Phylogenet. Evol.* 79, 215–230.
- Librado, P., Rozas, J., 2009. DnaSP v5: a software for comprehensive analysis of DNA polymorphism data. *Bioinformatics* 25, 1451–1452.
- Linder, H.P., de Klerk, H.M., Born, J., Burgess, N.D., Fjeldsø, J., Rahbek, C., 2012. The partitioning of Africa: statistically defined biogeographical regions in sub-Saharan Africa. *J. Biogeogr.* 39, 1189–1205.
- Lorenzen, E.D., Heller, R., Siegmund, H.R., 2012. Comparative phylogeography of African savannah ungulates. *Mol. Ecol.* 21, 3656–3670.
- Lovett, J.C., 1993. Climatic history and forest distribution in eastern Africa. In: Lovett, J.C., Wasser, S.K. (Eds.), *Biogeography and Ecology of the Rain Forests of Eastern Africa*. Cambridge University Press, Cambridge, UK, pp. 23–29.
- Matzke N.J., 2013a. Package ‘BioGeoBEARS’.
- Matzke, N.J., 2013b. Probabilistic historical biogeography: new models for founder-event speciation, imperfect detection, and fossils allow improved accuracy and model-testing. *Front. Biogeogr.* 5, 242–248.
- Matzke, N.J., 2014. Model selection in historical biogeography reveals that founder-event speciation is a crucial process in island clades. *Syst. Biol.* 63, 951–970.
- Measey, G.J., Vences, M., Drewes, R.C., Chiari, Y., Melo, M., Bourles, B., 2007. Freshwater paths across the ocean: molecular phylogeny of the frog *Ptychadena newtoni* gives insights into amphibian colonization of oceanic islands. *J. Biogeogr.* 34, 7–20.
- Medina, M.F., Bauer, A.M., Branch, W.R., Schmitz, A., Conradie, W., Nagy, Z.T., Hibbitts, T.J., Ernst, R., Portik, D.M., Nielsen, S.V., Colston, T.J., Kusamba, C., Behangana, M., Rödel, M.-O., Greenbaum, E., 2016. Phylogeny and systematics of *Panaspis* and *Afroablepharus* skinks (Squamata: Scincidae) in the savannas of sub-Saharan Africa. *Mol. Phylogenet. Evol.* 100, 409–423.
- Meier, R., Shiyang, K., Vaidya, G., Ng, P.K.L., 2006. DNA barcoding and taxonomy in Diptera: a tale of high intraspecific variability and low identification success. *Syst. Biol.* 55, 715–728.
- Merow, C., Smith, M.J., Silander, J.A., 2013. A practical guide to MaxEnt for modeling species’ distributions: what it does, and why inputs and settings matter. *Ecography* 36, 1058–1069.
- Miller, J.M., Hallager, S., Monfort, S.L., Newby, J., Bishop, K., Tidmus, S.A., Black, P., Houston, B., Matthee, C.A., Fleischer, R.C., 2010a. Phylogeographic analysis of nuclear and mtDNA supports subspecies designations in the ostrich (*Struthio camelus*). *Conserv. Genet.* 12, 423–431.
- Miller, M.A., Pfeiffer, W., Schwartz, T., 2010b. Creating the CIPRES Science Gateway for Inference of Large Phylogenetic Trees. In: *Gateway Computing Environments Workshop (GCE)*, New Orleans, LA, pp. 1–8.
- Miralles, A., Carranza, S., 2010. Systematics and biogeography of the Neotropical genus *Mabuya*, with special emphasis on the Amazonian skink *Mabuya nigropunctata* (Reptilia, Scincidae). *Mol. Phylogenet. Evol.* 54, 857–869.
- Njabo, K.Y., Bowie, R.C.K., Sorenson, M.D., 2008. Phylogeny, biogeography and taxonomy of the African wattle-eyes (Aves: Passeriformes: Platysteiridae). *Mol. Phylogenet. Evol.* 48, 136–149.
- Outlaw, R.K., Voelker, G., Outlaw, D.C., Klicka, J., 2007. Molecular systematics and historical biogeography of the Rock-Thrushes (Muscicapidae: *Monticola*). *Auk* 124, 561–577.
- Pabijan, M., Brown, J.L., Chan, L.M., Rakotondravony, H.A., Raselimanana, A.P., Yoder, A.D., Glaw, F., Vences, M., 2015. Phylogeography of the arid-adapted Malagasy bullfrog, *Laliostoma labrosum*, influenced by past connectivity and habitat stability. *Mol. Phylogenet. Evol.* 92, 11–24.
- Palumbi, S.R., 1996. Nucleic acids II: the polymerase chain reaction. In: Hillis, D.M., Moritz, C., Mable, B.K. (Eds.), *Molecular Systematics*. second ed. Sinauer, Sunderland, Massachusetts, pp. 205–247.
- Penner, J., Wegmann, M., Hillers, A., Schmidt, M., Rödel, M.-O., 2011. A hotspot revisited – a biogeographical analysis of West African amphibians. *Divers. Distrib.* 17, 1077–1088.
- Peterson, A.T., Nyári, Á.S., Crandall, K., 2008. Ecological niche conservatism and Pleistocene Refugia in the Thrush-like Mourner, *Schiffornis* sp., in the Neotropics. *Evolution* 62, 173–183.
- Peterson, T.A., Soberón, J., Pearson, R.G., Anderson, R.P., Martínez-Meyer, E., Nakamura, M., Araújo, M.B., 2011. *Ecological Niches and Geographic Distributions*. Princeton University Press, Oxford.
- Phillips, S.J., Anderson, R.P., Schapire, R.E., 2006. Maximum entropy modeling of species geographic distributions. *Ecol. Model.* 190, 231–259.
- Phillips, S.J., Dudík, M., 2008. Modeling of species distributions with Maxent: new extensions and a comprehensive evaluation. *Ecography* 31, 161–175.
- R Core Development Team, 2014. *R: A Language and Environment for Statistical Computing*. The R Foundation for Statistical Computing, Vienna, Austria.
- Rambaut, A., 2014a. FigTree Version 1.4.2.
- Rambaut, A., 2014b. Tracer v1.6 Available from <<http://beast.bio.ed.ac.uk/Tracer>>.
- Rato, C., Harris, D.J., Perera, A., Carvalho, S.B., Carretero, M.A., Rödder, D., 2015. A combination of divergence and conservatism in the niche evolution of the Moorish Gecko, *Tarentola mauritanica* (Gekkota: Phyllodactylidae). *PLoS ONE* 10, e0127980.
- Raxworthy, C.J., Pearson, R.G., Zimkus, B.M., Reddy, S., Deo, A.J., Nussbaum, R.A., Ingram, C.M., 2008. Continental speciation in the tropics: contrasting biogeographic patterns of divergence in the *Uroplatus* leaf-tailed gecko radiation of Madagascar. *J. Zool.* 275, 423–440.
- Ree, R.H., Smith, S.A., 2008. Maximum likelihood inference of geographic range evolution by dispersal, local extinction, and cladogenesis. *Syst. Biol.* 57, 4–14.
- Ronquist, F., 1997. Dispersal-vicariance analysis: a new approach to the quantification of historical biogeography. *Syst. Biol.* 46, 195–203.
- Ronquist, F., Teslenko, M., van der Mark, P., Ayres, D.L., Darling, A., Höhna, S., Larget, B., Liu, L., Suchard, M.A., Huelsenbeck, J.P., 2012. MrBayes 3.2: efficient Bayesian phylogenetic inference and model choice across a large model space. *Syst. Biol.* 61, 539–542.
- Sabaj, M.H., 2016. Standard Symbolic Codes for Institutional Resource Collections in Herpetology and Ichthyology: An Online Reference Version 6.5 (16 August 2016). Electronically accessible at <<http://www.asih.org/>>. American Society of Ichthyologists and Herpetologists, Washington, DC.
- Sievers, F., Wilm, A., Dineen, D., Gibson, T.J., Karplus, K., Li, W., Lopez, R., McWilliam, H., Remmert, M., Söding, J., Thompson, J.D., Higgins, D.G., 2011. Fast, scalable generation of high-quality protein multiple sequence alignments using Clustal Omega. *Mol. Syst. Biol.* 7, 539.
- Smits, N., Berthouly, C., Cornélis, D., Heller, R., Van Hooft, P., Chardonnet, P., Caron, A., Prins, H., van Vuuren, B.J., De longh, H., Michaux, J., 2013. Pan-African genetic structure in the African Buffalo (*Syncerus caffer*): investigating intraspecific divergence. *PLoS ONE* 8, e56235.
- Stamatakis, A., 2014. RAXML version 8: a tool for phylogenetic analysis and post-analysis of large phylogenies. *Bioinformatics* 30, 1312–1313.
- Swets, J.A., 1988. Measuring the accuracy of diagnostic systems. *Science* 240, 1285–1293.
- Swofford, D.L., 2001. PAUP. Phylogenetic Analysis Using Parsimony (* and Other Methods) Version 4. Sinauer Associates, Sunderland, Massachusetts.
- Templeton, A.R., Crandall, K.A., Sing, C.F., 1992. A cladistic analysis of phenotypic associations with haplotypes inferred from restriction endonuclease mapping and DNA sequence data. III. Cladogram estimation. *Genetics* 132, 619–633.
- Venables, W.N., Ripley, B.D., 2002. *Modern Applied Statistics with S*. Springer, New York, NY, USA.
- Vences, M., Kosuch, J., Rödel, M.-O., Lötters, S., Channing, A., Glaw, F., Böhme, W., 2004. Phylogeography of *Ptychadena mascareniensis* suggests transoceanic dispersal in a widespread Africa-Malagasy frog lineage. *J. Biogeogr.* 31, 593–601.
- Voelker, G., Outlaw, R.K., Bowie, R.C.K., 2010. Pliocene forest dynamics as a primary driver of African bird speciation. *Glob. Ecol. Biogeogr.* 19, 111–121.
- Voelker, G., Penabaz, J.V., Huntley, J.W., Bowie, R.C., 2014. Diversification in an Afro-Asian songbird clade (*Erythropgia-copsychus*) reveals founder-event speciation via trans-oceanic dispersals and a southern to northern colonization pattern in Africa. *Mol. Phylogenet. Evol.* 73, 97–105.

- Warren, D.L., Glor, R.E., Turelli, M., 2010. ENMTTools: a toolbox for comparative studies of environmental niche models. *Ecography* 33, 607–611.
- Warren, D.L., Seifert, S.N., 2011. Ecological niche modeling in Maxent: the importance of model complexity and the performance of model selection criteria. *Ecol. Appl.* 21, 335–342.
- Wickham, H., 2009. *Ggplot2: Elegant Graphics for Data Analysis*. Springer, New York, NY, USA.
- Wiens, J.J., 2011. The niche, biogeography and species interactions. *Philos. Trans. R. Soc. B: Biol. Sci.* 366, 2336–2350.
- Wiens, J.J., Graham, C.H., 2005. Niche conservatism: integrating evolution, ecology, and conservation biology. *Annu. Rev. Ecol. Evol. Syst.* 36, 519–539.
- Wilcox, T.P., Zwickl, D.J., Heath, T.A., Hillis, D.M., 2002. Phylogenetic relationships of the dwarf boas and a comparison of Bayesian and bootstrap measures of phylogenetic support. *Mol. Phylogenet. Evol.* 25, 361–371.
- Zhang, J., Kapli, P., Pavlidis, P., Stamatakis, A., 2013. A general species delimitation method with applications to phylogenetic placements. *Bioinformatics* 29, 2869–2876.
- Zimkus, B.M., Rödel, M.-O., Hillers, A., 2010. Complex patterns of continental speciation: molecular phylogenetics and biogeography of sub-Saharan puddle frogs (*Phrynobatrachus*). *Mol. Phylogenet. Evol.* 55, 883–900.